INTERPRETING OROGRAPHIC SNOWFALL PATTERNS

BY

J. OWEN RHEA

Atmospheric Science
PAPER NO.
197

DEPARTMENT OF ATMOSPHERIC SCIENCE
COLORADO STATE UNIVERSITY
FORT COLLINS, COLORADO

ABSTRACT

Winter precipitation in mountainous southwest Colorado was related to terrain slope and elevation by multiple regression. From a 12 season record of 15 daily precipitation stations, the study used only those days with ≥ .01 in. at ≥ one station. Days used were classed by mean 24 hour 700mb wind direction and speed. By class, each station's mean 24 hour precipitation was computed as was station slope over 8 distances. These precipitation values were correlated to elevation and to products of terrain slope X 700mb wind speed X 700mb mean saturation mixing ratio lapse rate. (Products are simplified factors in an orographic precipitation formula.)

Multiple correlation coefficient ranged between 0.80 and 0.98 for both speed and direction constant and was 0.68 for both variable. Correlation to elevation was negligible. Thus, slope explained most of the areal precipitation distribution. For each of two test years, correlation between computed and observed seasonal precipitation was ≥ 0.92. Technique refinement into a short term predictor seems feasible.

ACKNOWLEDGEMENTS

Numerous individuals have offered encouragement and helpful suggestions contributing to the successful completion of this study. In particular, thanks are due my advisor, Dr. James Rasmussen for his patience, counsel and encouragement. Also, I wish to acknowledge the many contributions made by all my colleagues, past and present, through mutual discussion (technical or philosophical) and participation in Colorado winter meteorological field projects. I am especially grateful to Dr. Larry G. Davis, who provided me the opportunity to continue my education. Mr. Dave Blanchar played a most vital part by adapting the data for computer processing and executing the programs. My wife, Rosemary, was particularly patient and understanding and offered many helpful comments on the format and content of the text. Finally, thanks are due Mrs. Kay Leach, Cheryl Allsebrook and especially Miss Suzanne Curry and Miss Sue Wood for typing of the manuscript and to Mrs. Micki Carleton and Roberta Kooy for drafting of the figures.

Publication of this report was supported by the State of Colorado Experiment Station under Project No. 15-1371-1113 and by the U. S. Department of Interior, Bureau of Reclamation, under Contract No. 14-06-D-6963 to E. G. & G., Inc.

TABLE OF CONTENTS

TABLE OF CONTENTS (Continued)

1.0 INTRODUCTION

1.1 Purpose

Accurate current and predictive knowledge of both point and areal winter precipitation in mountainous regions is of considerable importance to a wide range of the population. The attainment of such knowledge is lagging advances in weather prediction being made in certain other areas. The influence of terrain on precipitation in mountainous regions is readily recognized, but quantifying the effect remains difficult, as the overall process is quite complex.

The purpose of this paper is to contribute to the knowledge of terrain effect by relating precipitation specifically to terrain slope under varying wind regimes.

1.2 Discussion

Many hydrologic studies have used the observational fact that precipitation generally increases with elevation as a point of departure to develop local linear regression relationships between precipitation and elevation. Interesting examples of this approach can be found in Peck and Brown (1962) for Utah and Hounam (1958) for a part of Australia. A frequent observational comment from such studies is that the relationships hold only for a relatively localized area and work particularly well for areas with similar terrain aspect. A good example of this is shown by Figure 1, from Marlatt and Riehl (1963).

Mathematically, the terrain-induced (orographic) potential precipitation is proportional to $\frac{\partial qs}{\partial Z} \cdot (\vec{\nabla}_Z \cdot \vec{V}_h)$ where $\vec{V}_h$ is horizontal wind, $\vec{\nabla}_Z$ is the terrain gradient, and $\frac{\partial qs}{\partial Z}$ is the local change of saturation mixing ratio with height. A more complete relationship is developed in Section 3.1.3.

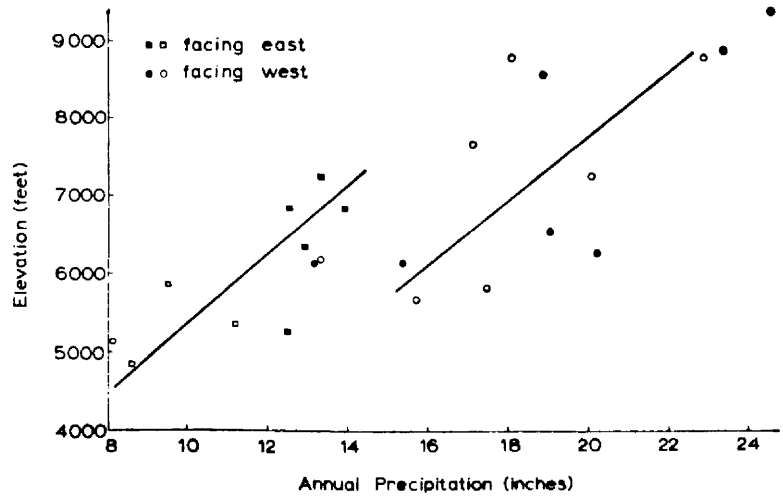

Figure 1. Average annual precipitation as a function of elevation and aspect. Solid dots or squares refer to 13 stations over the Colorado River Basin (Marlatt and Riehl, 1963).

The total precipitation process is compounded, however, because it is frequently made up of components from (a) large-scale vertical motion fields arising from migratory waves, (b) orographic (terrain) lifting, and (c) local release of conditional instability (convection) as pointed out by Elliott and Shaffer (1962), Hjermstad (1970), Chappell (1970), and others. Each of these factors is quite important during the period of time over which it is acting. Rasmussen (1963) explained up to 25% of the variance in seasonal precipitation over the Colorado River Basin by using multiple correlation to a number of circulation features. He (Rasmussen, 1968) explained up to 64% of the variance on a storm period basis using a more complete atmospheric water budget approach.

In many high, complex terrain areas, the terrain influence exerts the dominant control, however, because it provides (1) a more persistent orographic vertical motion field and (2) a forced lifting zone

for release of convection. Ridge-to-valley winter precipitation ratios are observed to range mainly between 2 and 10/1 (Hjermstad, 1970; Rogers, 1970; Rhea, 1967; Elliott and Shaffer, 1962; Peck and Williams, 1962). These ratios show large variability however over short time periods due partially to the passage of meso-scale convergence bands (periodicity of 3-5 hours) as observed by Elliott and Hovind (1964) in California and by Rhea, et al. (1969) in Colorado at much higher altitudes.

Numerous other factors complicate the specification of point precipitation, especially for snowfall, not the least of which are (1) the rather complex effects of wind and temperature on dendritic (high mass) snow crystal initiation altitudes and subsequent trajectories, (2) the presence of interference patterns (constructive or destructive) between multiple mountain waves over complex terrain, and (3) increasingly large errors in snowfall measurement as wind increases, thus precluding accurate knowledge of historical values of precipitation for calibrating predictive models.

Despite these complexities, mountain precipitation regimes can be studied systematically with the objective of assessing the importance of a given precipitation contributing factor. This paper henceforth concentrates on the orographic (terrain-slope) factor.

2.0 REVIEW OF RELATED STUDIES

Spreen (1947) indirectly partially accounted for variations in the orographic precipitation expression (given in equation 3.7 of Section 3.1.3) and explained up to 88% of the variance in winter precipitation between selected stations over western Colorado through graphical multiple correlation to the following terrain factors: elevation, maximum terrain slope within 5 miles of the station, exposure (relative freedom from obstructing barriers within 20 miles), and orientation of exposure. He did not attempt to directly relate these factors to any causal meteorological flow parameters.

Chappell (1970) computed supply rate of condensate by assuming certain mean values of orographic vertical motion and $\frac{\partial qs}{\partial z}$ through the estimated cloud depth for Wolf Creek Pass and Climax, Colorado. Quite good agreement to observed average precipitation was obtained (except for the warmest temperatures) when also accounting for theoretical changes in nucleation efficiency for converting the condensate to precipitation.

Elliott and Shaffer (1962) used a similar formulation to that for orographic precipitation in Section 3.1.1 and California coastal soundings for data input. They obtained single correlation coefficients between 0.44 and 0.63 for observed versus calculated hourly precipitation in the San Gabriel and Santa Ynez Mountains. Higher r-values of 0.5 to 0.8 were obtained when replacing the theoretical equation with a multiple regression formula with parameters of stability, temperature (and therefore condensate supply rate), and wind speed and direction

as the independent variables. Finally, when empirically accounting for the non-orographic precipitation component r-values ranged from 0.67 to 0.94.

A most interesting study by Kusano, et al. (1957) in Japan, made direct use of the orographic precipitation equation (including height dependent damping factor) for summer orographic rainfall. Values of rainfall were obtained graphically by using an overlay on a terrain map and considering wavelengths of 60, 120 and 300 km. Excellent improvement of calculated versus observed precipitation amount and distribution was obtained compared to the calculations by the Estoque model .

Parameterized numerical modeling of orographic precipitation over an idealized barrier has been accomplished by Sarker (1967) for rain in the Western Ghats of India and by Willis (1970) whose test data was from snowfall precipitation over the Park Range in northwest Colorado. Sarker obtained very good rainfall profile agreement to observed values while Willis found consistent agreement on the upwind side of the mountain only when a number of snow fall cases were averaged together. This difference in model results is perhaps a manifestation that the much smaller terminal velocities of snow crystals considerably complicates the real distribution of snow deposition and also decreases the snow measurement accuracy compared to rain.

Finally, a preliminary study of the 700 mb wind direction dependence of meso-scale precipitation patterns in western Colorado by Rhea, et al. (1969) led to the present study which takes direct account of the effect of terrain slope on precipitation through a multiple regression scheme.

3.0 DESIGN OF THE STUDY

3.1 Theoretical Considerations

In mountainous terrain, total precipitation can generally be attributed to vertical velocities w_d, w_c, and w_o arising from (1) large-scale convergence (negative divergence), (2) convection, and (3) orographic lifting as discussed briefly in Section 1.2. Symbolically, this can be expressed as:

$$R_t = R_d(w_d(z),\ q(z),\ T(z),\ t) + R_c(w_c(z),\ q(z),\ T(z),\ t) + R_o(w_o(z),\ q(z),\ T(z),\ t) \tag{3.1}$$

i.e., total precipitation, R_t is a function not only of the three vertical motion profiles but also of vertical profiles of mixing ratio, $q(z)$ and temperature, $T(z)$ and also the duration, t, of the processes. Subscripts, d, c and o, refer to divergence, convection and orographic respectively.

3.1.1 Large Scale Convergence

Numerous formulations to quantify R_d exist. Many of these compute the vertical velocity using horizontal divergence of the wind field, the continuity equation, and certain assumptions on compressibility. Divergence, in turn, is directly proportional to the rate of change of the vertical component of vorticity, $\dot{\zeta}$. Values of w_d computed are generally in the range of 1 to 5 cm sec^{-1}. Precipitation rates therefrom are computed and observed to be between 0.01 and 0.1 in. hr^{-1} during winter over high, mountainous regions while the convergence condition exists. Accuracy limitation arises chiefly from the meteorologically universal problem of inadequate input data resolution. Since this paper is primarily concerned with studying R_o, no

further elaboration on R_d will be made. Its direct proportionality to $\dot{\zeta}$, however, should be noted for future reference in Section 4.

3.1.2 Convection

The convective vertical motion w_c can be fairly well computed for individual cumulus clouds of a given radius when accurate knowledge of environmental temperature, mixing ratio and wind profiles exists. Computation can be made from versions of either steady-state models of cumulus convection developed by Weinstein and Davis (1967) and Simpson (1968) or time-dependent models such as that of Weinstein (1968). These models yield sufficiently accurate computations of cloud-top (r = 0.8 to 0.9) and precipitation (r = 0.6 to 0.8) to have been incorporated as valuable tools in execution and evaluation of cumulus weather modification projects (Davis, et al., 1968; Simpson, 1970). Computed w_c values for the type of marginal instability existing in winter over mid-latitude mountainous regions range from 50 to 250 cm sec^{-1} and precipitation computes at 0.05 to 0.25 in. hr^{-1}, values which are realistic over short periods of time. Major difficulty is encountered, however, in accurately predicting (1) profiles of temperature, humidity and wind such that the existence and effect of marginal instability can be assessed, and (2) areal coverage and duration of convective precipitation if it does exist. Variability and predictability of R_c is thus a substantial hindrance to systematically accounting for R_t or studying either R_d or R_o.

3.1.3 Orographic Precipitation

The orographic precipitation r_o produced from a mass of air, dm, is very closely approximated by

$$r_o = E \left(\frac{\partial qs}{\partial z}\right) \cdot w_o \cdot dm \cdot dt \qquad (3.2)$$

where

E = efficiency of converting condensed cloud water to precipitation

$\frac{\partial q_s}{\partial z}$ = local (parcel) change in saturation mixing ratio with height

w_o = orographic vertical motion of mass, dm, over time, dt

By definition, the pressure, P, of a column of air is the air weight, mg, per unit area. Therefore,

$$dm = A\frac{dP}{g} \tag{3.3}$$

where A = cross-sectional area.

Equation (3.2) can then be written in traditional units of precipitation water depth as

$$r_o = \frac{AE}{A\rho_w}\left(\frac{\partial q_s}{\partial z}\right) \cdot w_o \cdot \frac{dP}{g} \cdot dt \tag{3.4}$$

where ρ_w = density of water.

Integration is required to obtain total orographic precipitation, R_o, i.e.

$$R_o = \frac{E}{\rho_w g}\int_t \int_P \left(\frac{\partial q_s}{\partial z}\right) \cdot w_o \cdot dP \cdot dt \tag{3.5}$$

For a saturated adiabatic process an analytic thermodynamic expression exists for $\frac{\partial q_s}{\partial z}$; also, the profile of w_o over idealized, smooth barriers can be approximated by solution of a differential equation, with barrier shape and dimension, stability, and vertical windshear as equation variables. $w_o(z)$ can also be approximated by applying an exponential damping factor, f(z), (Kusano, et al., 1957; Berkofsky, 1964) to the orographic vertical motion value, $w_{o\ell}$, produced by the impingement of the low-level wind, $\vec{V}_\ell$, against the barrier with slope, $\vec{\nabla}z$, to yield an expression for w_o at height, z, of:

$$w_{o(z)} = f(z)\, w_{o\ell} = f(z) \cdot (\vec{\nabla}z \cdot \vec{V}_\ell) \tag{3.6}$$

Substitution into Eq. (3.5) yields

$$R_o = \frac{E}{\rho_w g} \int_t \int_P f(z) \cdot \frac{\partial qs}{\partial z} \cdot (\vec{\nabla}z \cdot \vec{V}_\ell)\, dP\, dt \tag{3.7}$$

Specifying the location at which R_o will be deposited is very difficult, especially for snowfall in rugged terrain due partially to low terminal velocities (0.4 to 1.3 m sec^{-1}) of snow crystals (Brown, 1970) which are being carried through a complicated field of w_o (0.1 to 0.7 m sec^{-1}) arising from multiple mountain waves.

3.2 Experimental Approach

This study assumes E and f(z) in Eq. (3.7) to be invariant and makes no attempt to treat them specifically. It also makes no attempt at directly integrating Eq. (3.7). Rather, a statistical approach is taken to relate average station precipitation to variations in the product $\frac{\partial qs}{\partial z} \cdot (\vec{\nabla}z \cdot \vec{V}_\ell)$. A brief attempt is made to account for variations in saturated column pressure depth, $\int_P dP = \Delta P$, and duration, $\int_t dt = \Delta t$, in section 4.4.

Specifically, the experiment was designed to systematically study the effect of varying wind direction and speed (and the resulting variation in $\frac{\partial qs}{\partial z} \cdot (\vec{\nabla}z \cdot \vec{V}_\ell)$ on snowfall precipitation at a given point. The San Juan Mountain region of southwestern Colorado was chosen as the setting for the study (Figure 2). The 700 mb level (which is found at or below barrier height) was chosen as the key level for extracting values of $\overline{(\frac{\partial qs}{\partial z})}_{700}$ and the real wind, $\overline{\vec{V}}_{700} = \vec{V}_\ell$. The first part of the study displays the resulting wind direction-dependent precipitation patterns in map form, while the second and more definitive part statistically relates precipitation values to the product of terrain slope,

wind speed, and $\left(\frac{\partial q_s}{\partial z}\right)_{700}$ through least squares linear multiple regression.

3.3 Data

The basic data used was:

(1) Vector average 700 mb wind direction for Grand Junction, Colorado, (Figure 3) for the 24 hour precipitation period in question.

(2) Mean 700 mb wind speed for Grand Junction for the 24 hour period.

(3) 700 mb 24 hour mean temperature for Grand Junction.

(4) Records from 20 NOAA climatological (non-recording) 24 hour precipitation stations (Table 1 and Figure 2) with reading times near sunset (or 0000Z).

(5) Topographic maps (1:250,000) for the area from which elevations were tabulated at 10 km intervals out to 50 km upstream and downstream from the station in question for designated 700 mb wind direction categories.

Data records studied were November through March, 1955-56 through 1966-67. The seasons 1967-68 and 1968-69 were held out as test data.

In addition to the above set of basic data, the Steamboat Springs precipitation record and terrain profiles were used as test data as were terrain profiles for two points near Silverton.

3.4 Data Treatment

3.4.1 Precipitation Days

First, the sample studied was restricted to days on which measurable precipitation was recorded at at least one of the 20 stations thus eliminating totally dry days.

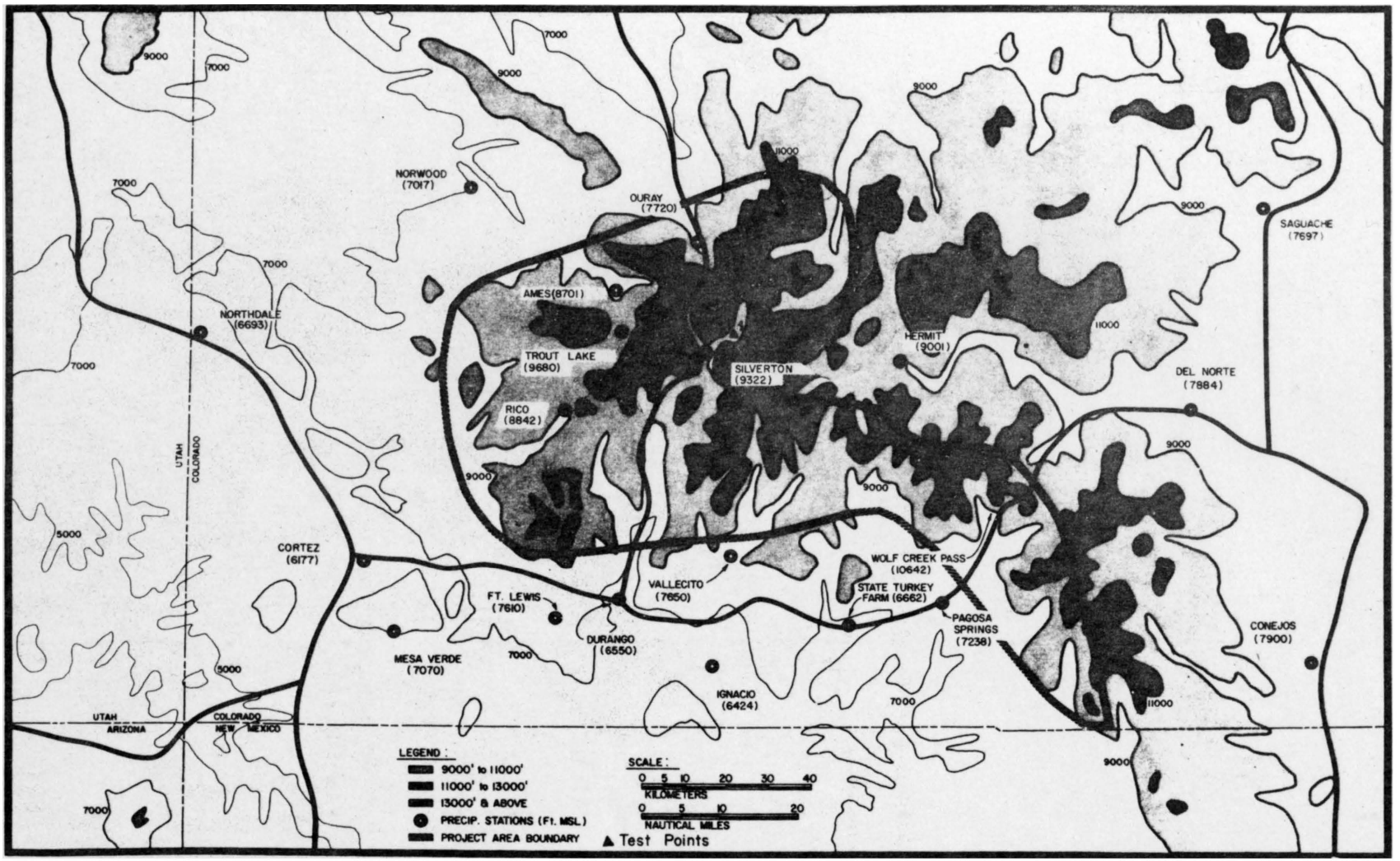

Figure 2. Topography and precipitation station locations in the study area (E.G.&G., 1970)

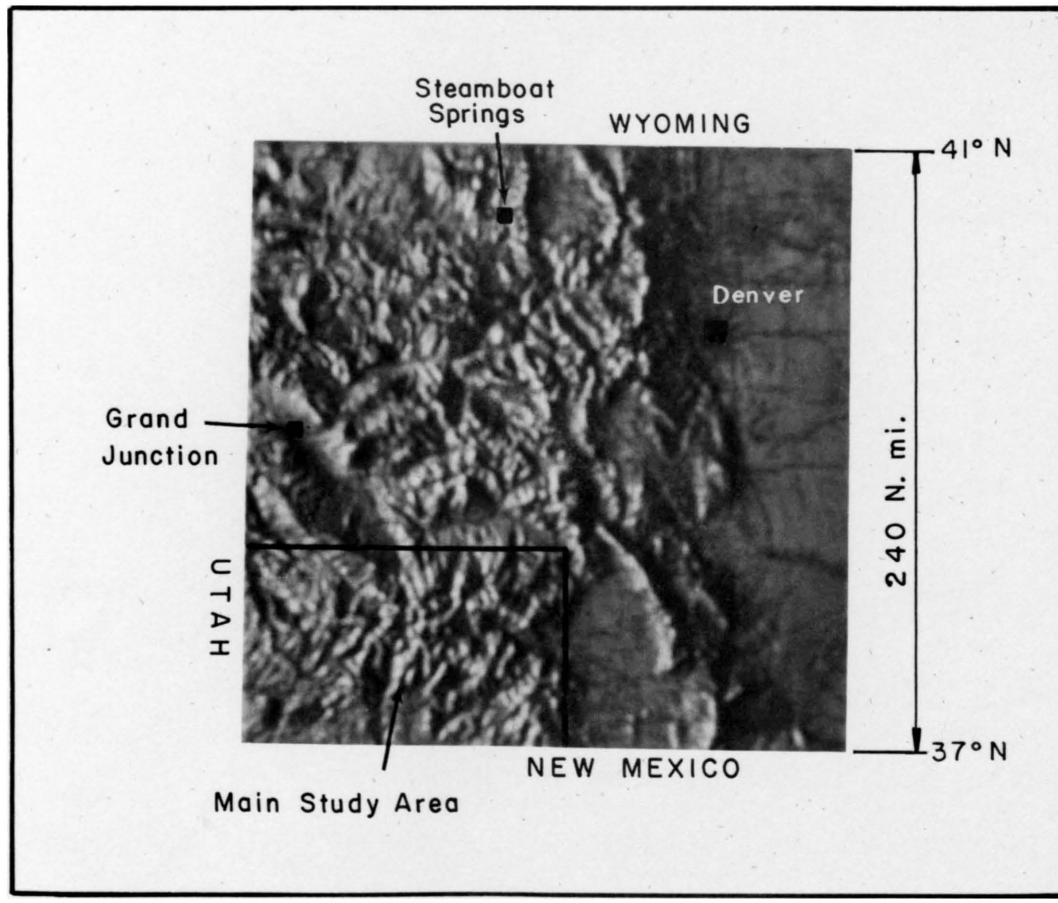

Figure 3. Larger area map showing Grand Junction, Steamboat Springs, and the main study area.

3.4.2 700 mb Data

Second, the vector mean 700 mb wind directions at Grand Junction were computed (using 00Z, 12Z, 00Z values) to bracket the precipitation day, for each of the resulting "precipitation days" from above. Corresponding mean 700 mb temperature and wind speed were also calculated.

3.4.3 Direction Stratification

Next, twelve 30° direction categories were designated running clockwise consecutively from 175° - 204°, 205° - 234°, to 145° - 174°, and labeled categories 1 through 12, respectively. The precipitation data set was stratified accordingly.

3.4.4 Speed Stratification

Each direction-stratified precipitation data set was then sub-stratified by 700 mb wind speed into the six categories shown in Table 2.

3.4.5 Precipitation Averaging

For the first part of the study $(\overline{R}_t)_{i,k}$ (average 24 hour precipitation) for station k in direction i class were computed for i = 1, 2, ..., 12 along with the overall average $(\overline{R}_t)_k$ for each station regardless of direction.

For the more detailed study, average 24 hour precipitation, $(\overline{R}_t)_{i,j,k}$, for station, k, in direction i and speed j categories were also calculated and the Grand Junction average 700 mb temperature, $\overline{T}_{i,j}$, was also thus tabulated (Table 3). Note that there are 27 i, j joint stratifications with greater than zero frequency of occurrence. Also, only 15 of the stations had adequate record quality to be used in this part of the study.

TABLE 1

Precipitation Stations Used in the Study

Station	No.	Elevation (m)	Station	Elevation (m)
Ames	1	2610	Conejos	2370
Cortez	2	1853	Saguache	2310
Del Norte	3	2365	St. Turkey Farm	1999
Durango	4	1965	Trout Lake	2904
Ft. Lewis	5	2278	Wolf Creek Pass	3193
Hermit	6	2700		
Ignacio	7	1927		
Mesa Verde	8	2121		
Northdale	9	2008		
Norwood	10	2105		
Ouray	11	2322		
Pagosa Spgs.	12	2171		
Rico	13	2653		
Silverton	14	2797		
Vallecito	15	2295		

TABLE 2

700 mb Wind Speed Classes

j - index	1	2	3	4	5	6
Range (kts)	6-12	13-18	19-24	24-30	31-36	$\geq$37

TABLE 3

Station Average 24 Hour Precipitation By 700mb Wind Direction and Speed Categories

(Precipitation values are in thousandths of inches)

Direction Category Number	1			2				3					
Degrees	175-204			205-234				265-294					
Speed Category Number	1	2	4	1	2	3	4	1	2	3	4	5	6
Kts.	6-12	13-18	25-30	6-12	13-18	19-24	25-30	6-12	13-18	19-24	25-30	31-36	37-42
No. of Precip. Days	18	13	6	17	35	20	12	28	67	34	22	7	3
1. A Ames	070	105	198	244	180	296	458	142	168	210	216	315	610
2. B Cortez	140	139	107	089	177	151	111	080	087	127	098	104	140
3. C Del Norte	240	045	000	054	076	034	043	014	018	022	020	000	083
4. D Durango	240	209	352	206	324	314	361	119	109	188	223	240	593
5. E Ft. Lewis	200	198	283	131	276	207	441	088	119	145	179	114	397
6. F Hermit	130	158	233	076	127	127	155	084	063	075	152	029	283
7. G Ignacio	100	177	178	141	162	283	108	067	064	085	122	225	147
8. H Mesa Verde	200	265	215	121	262	262	294	119	124	176	173	147	313
9. I Northdale	060	173	180	160	202	108	156	051	060	079	121	128	200
10. J Norwood	110	091	038	105	152	094	079	114	089	077	069	076	137
11. K Ouray	090	120	140	120	114	127	175	118	120	119	131	079	157
12. L Pagosa	270	224	298	178	182	308	308	111	112	246	252	256	573
13. M Rico	100	229	290	170	279	370	610	140	186	253	271	478	683
14. N Silverton	104	182	294	110	243	234	235	124	121	152	165	252	467
15. O Vallecito	280	298	407	338	372	362	402	183	171	236	300	367	820
Mean 700MB Temp.	-5.2	-5.1	-3.0	-6.5	-6.1	-4.2	-4.2	-7.3	-6.7	-5.8	-4.2	-4.6	-5.0

Direction Category As Above	4				5				6			7		
	265-294				295-324				325-354			355-024		
Speed Category As Above	1	2	3	4	1	2	3	4	1	2	33	1	2	3
	6-12	13-18	19-24	25-30	6-12	13-18	19-24	25-30	6-12	13-18	19-24	6-12	13-18	19-24
No. of Precip. Days	34	76	44	9	27	41	20	7	20	25	4	18	19	4
1. A	125	114	151	066	140	117	080	067	043	058	103	059	064	033
2. B	068	056	049	020	020	021	032	001	012	017	018	042	002	008
3. C	024	011	018	011	032	020	015	004	018	051	200	056	031	030
4. D	071	038	052	062	021	021	023	007	006	024	073	040	005	013
5. E	060	055	072	037	030	030	030	000	010	038	000	028	010	000
6. F	058	022	041	017	027	018	033	057	008	039	050	011	011	025
7. G	061	045	037	023	016	021	006	000	008	013	000	029	002	013
8. H	089	093	062	066	025	041	021	003	023	031	053	026	014	020
9. I	030	032	018	004	019	007	006	000	005	004	008	013	026	010
10. J	069	075	043	050	036	066	008	004	022	041	103	024	056	085
11. K	134	103	089	046	134	197	090	127	121	171	310	122	164	210
12. L	109	054	049	040	036	028	014	001	011	021	008	050	026	038
13. M	103	107	154	099	091	063	039	064	022	022		061	014	043
14. N	054	098	117	099	057	093	098	199	017	039	153	058	031	028
15. O	116	072	058	080	036	035	035	017	016	037	058	050	013	083
Mean 700MB Temp.	-9.9	-8.3	-7.0	-6.3	-8.1	-8.2	-7.0	-6.7	-11.2	-10.1	-10.8	-8.5	-9.5	-11.3

3.4.6 Terrain Slope Computations

Terrain slope $(\vec{\nabla}z)_{i,k\ell}$ computations for each station in direction category, i, were made by first computing mean elevation along a 30 degree arc at 10 km radius increments both upstream and downstream from the station out to 50 km. The procedure is shown in Figure 4. Figure 5 is an example of the resulting direction-dependent elevation profiles for Durango.

Slopes were computed by taking end-point elevation differences for the 8 distance scales shown in Table 4 and then dividing by the distance increment, ΔS. Rationale for selecting such a number of slope variables was that (1) snow crystal production and trajectories are influenced by a multiplicity of terrain-induced (orographic) vertical motion fields and (2) it would be desirable to determine which, if any, of the selected slope factors exhibited a consistently dominant influence on precipitation through high correlation. The problem of determining where best to measure terrain slope affecting precipitation at a point is complicated by the opposing effects of (1) the condition that in stably stratified flow the axis of maximum vertical motion slopes upwind with height and (2) masses of cloud-water and the resulting snow crystals produced from this region of maximum orographic vertical velocity are carried downwind toward the barrier.

3.5 Analysis Methods

3.5.1 Normalized Precipitation Maps

The ratio $\frac{(\overline{R}_t)_{i,k}}{(\overline{R}_t)_k}$ was computed for each station, where $(\overline{R}_t)_{i,k}$ is station k's average precipitation in direction i (for all speeds) and $(\overline{R}_t)_k$ is that station's overall average, regardless of wind direction, speed or any other stratification. Values of these

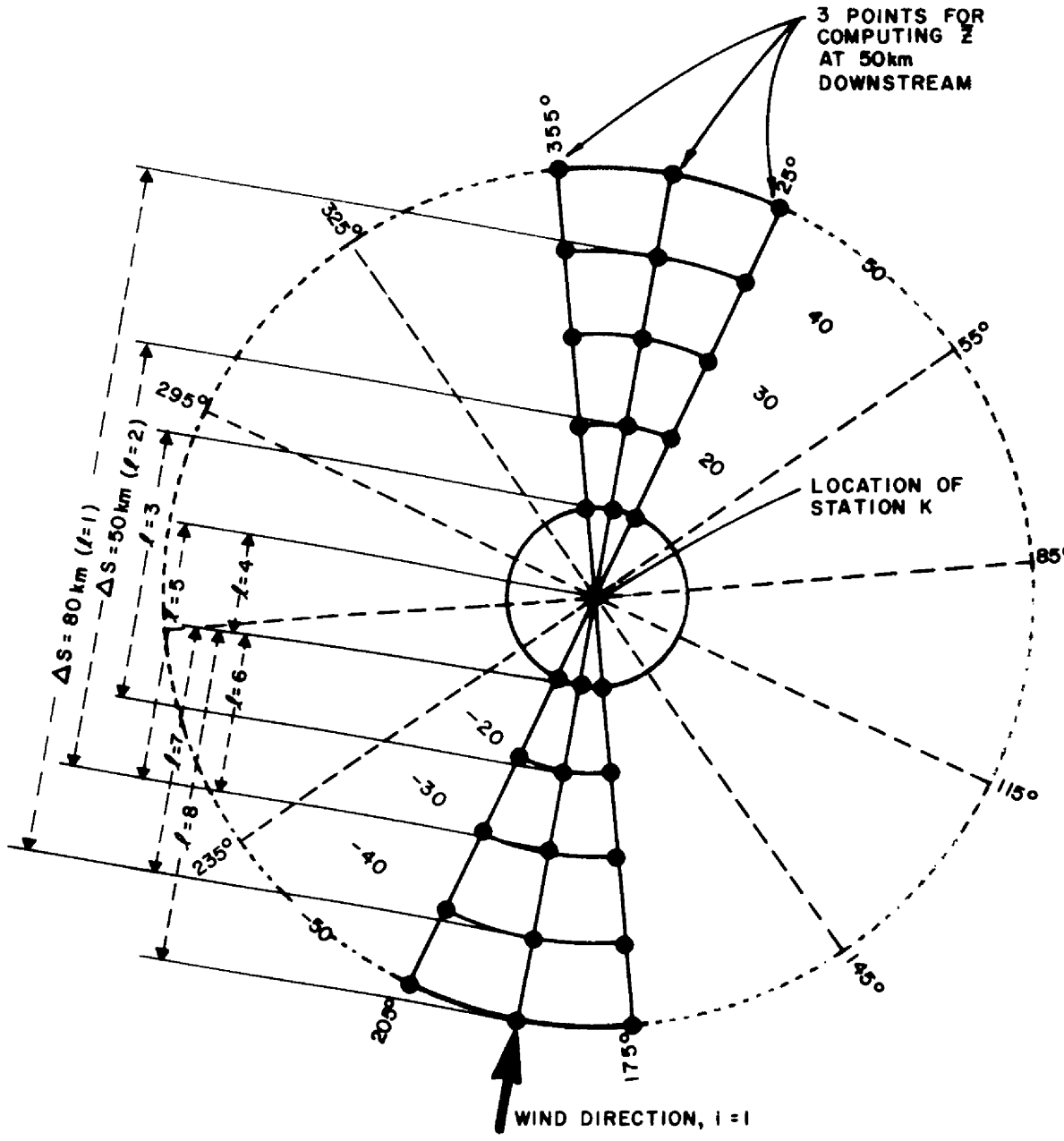

Figure 4. Schematic of methods for computing mean elevations and terrain slopes.

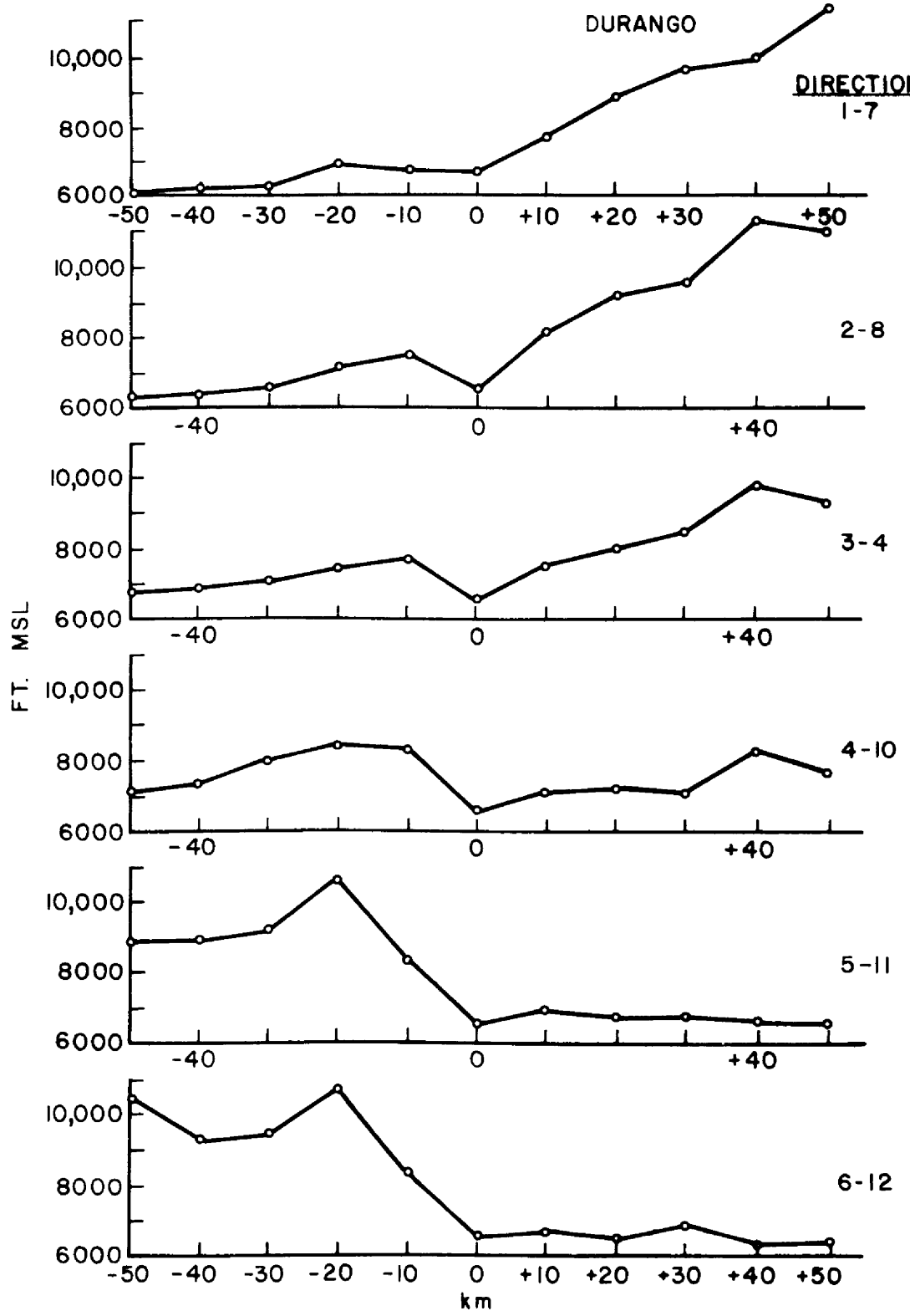

Figure 5. Average terrain profile encountered by air moving over Durango from left to right (right to left) for direction categories i = 1, ..., 6 (7-12) (E.G.&G., 1970).

TABLE 4

Distances Over Which Terrain Slope

Was Computed (See Figures 4 and 5)

$$(\nabla z)_{i,j} = [(z_2 - z_1)/\Delta s]_{i,j}$$

ℓ - Class	Location of z_2 (km)	Location of z_1 (km)	Δs (km)
1	+40	-40	80
2	+20	-30	50
3	+10	-20	30
4	0	-10	10
5	0	-30	30
6	-10	-30	20
7	-10	-40	30
8	-10	-50	40

dimensionless ratios can be contoured when plotted on an area map. This was done on maps showing topographic relief. Maps and pattern interpretation therefrom are presented in Section 4.1.

3.5.2 Statistical Treatment

By Equation (3.7), orographic precipitation at a point is theoretically proportional to the product of the mean local vertical change of saturation mixing ratio, with the scalar product of terrain slope and the low-level horizontal wind, i.e.,

$$R_o \propto \left(\overline{\frac{\partial q_s}{\partial z}}\right) \cdot (\vec{\nabla} z \cdot \vec{V}_\ell) \tag{3.8}$$

Unfortunately, it is difficult to isolate R_o from R_d and R_c (defined in Section 3.1). Therefore, this study for the most part

considered only R_t (where $R_t = R_d + R_c + R_o$) as the precipitation variable. Exceptions to this are found in Sections 4.2.4 and 4.4.3 where some attempt was made to separate R_o and $(R_d + R_c)$ and consider each in relation to possible causal factors. The major emphasis, then was on determining the validity of the proportionality (3.8) above when R_o was replaced by R_t.

Furthermore, according to the rationale expressed in Section 3.4.6 (concerning multiple fields of orographic vertical motion) it would be desirable to simultaneously consider the combined effects on precipitation of slope factors computed over several distance scales. To accomplish this, a statistical approach was taken through multiple linear regression analysis employing the method of least squares. A standard version of this routine was invoked (UCLA Bio-medical Statistical Series - BMDO2R).

The main object was to explain the observed inter-station variance among the values of average 24 hour precipitation, $(\overline{R}_t)_{i,j,k}$. Thus, the sample of dependent variables in each regression analysis consisted of one or more sets of the average precipitation data in Table 4. The exact choice depended upon the way in which direction, i, speed, j, and station, k, were allowed to vary (or remain constant). Table 5 lists the numerous ways in which the data sets were chosen for regression analysis; it also gives reasons for so choosing.

Nine terrain variables were chosen to correlate with station k's precipitation. These were station k's elevation and the eight terrain slope factors computed according to Table 4 (and multiplied by $(\overline{\frac{\partial qs}{\partial z}})_{700}$ and $|\vec{V}|_{700}$ according to proportionality (3.8)) with direction, i, also appropriately taken into account. Now, from the nature in which

TABLE 5

Data Sets of 12-Season Average 24 Hour Precipitation for Which Regression Equations Were Derived to Explain the Precipitation Variance in Relation to Elevation and Station Terrain Slope Factors Computed Over Eight Distance Scales (and Multiplied by $(\frac{\partial q_s}{\partial z})_{700\ mb}$ and $(|\vec{V}|)_{700\ mb}$ According to Proportionality (3.8).

Stratification Description	Each Case Sample Size	No. Eq. Derived	Indices	Section Where Discussed	Purpose
Speed and Direction Constant	15	27	i = constant, j = constant, k varies from 1 ... 15	4.2.1	To derive regression eqs. for the set of precipitation data holding wind direction, and speed constant, thus minimizing the greatest number of complicating factors
Wind Direction Constant, Speed Variable	45 - 90	7	i = constant j varies; 1, ..., 6 k varies; 1, ..., 15	4.2.2	To derive regression eqs. for the set of precipitation data keeping direction constant but letting speed vary to test the proportionality (3.8) over a range of wind speeds while minimizing influence of variations in large-scale factors
Direction, Speed and Temperature Variable	405	1	i = 1, ..., 7 j = 1, ..., 6 k = 1, ..., 15		To derive a general regression eq. applicable for all directions, all stations, at all speeds. Does not attempt to isolate non-orographic precipitation variability with direction
Direction, Speed and Temperature Variable; Non-orographic Components Isolated	105	1	i = 1, ..., 7 j = $\frac{2+3}{2}$ k = 1, ..., 15	4.2.4	Early attempt at same as immediately above except attempts to isolate non-orographic components and also account for variations in these with wind direction. Speed categories 2 and 3 were used as one class in computing precipitation data averages.
Direction, Speed and Temperature Variable; Non-orographic Components Isolated	405	1	i = 1, ..., 7 j = 1, ..., 6 k = 1, ..., 15	4.2.4	Same objective as immediately above but using the later data with the 27 Speed and Direction categories from Table 4.
Speed and Direction Constant, Station Variable	27	15	i = 1, ..., 7 j = 1, ..., 6 k = constant	4.2.5	To derive regression eq. for each station valid for all speeds and direction but accounting for local peculiarities of given station.

$(\vec{\nabla}z)_{i,k,l}$ is computed (stratified by i), it follows that:

$$(\vec{\nabla}z \cdot \vec{V}_\ell) = (\frac{z2-z1}{\Delta s})_{i,k,l} (|\vec{\bar{V}}|_{700})_{i,j} = (\frac{\Delta z}{\Delta s})_{i,k,l} \cdot (|\vec{\bar{V}}|_{700})_{i,j} \quad (3.9)$$

i.e, $\vec{\nabla}z$ and $\vec{V}_\ell$ are perfectly aligned by definition in this case and therefore the cosine of the angle between the vectors is 1.

Table 6 gives an example for the type of input data sets used for the regression analyses.

This then gives the following form to each resulting regression equation:

$$(\bar{R}_t)_{i,j,k,} = A_o + A_1 z_k + A_2[\nabla z_{i,k,1}(|\vec{\bar{V}}|_{700})_{i,j}(\overline{\frac{\partial qs}{\partial z}})_{700\ i,j}] + \cdots$$

$$+A_9[\nabla z_{i,k,8}(|\vec{\bar{V}}|_{700})_{i,j}\ (\overline{\frac{\partial qs}{\partial z}})_{700\ i,j}]$$

or

$$(\bar{R}_t)_{i,j,k} = A_o + A_1 z_k + [|\vec{\bar{V}}|_{700} \cdot (\frac{\partial qs}{\partial z})_{700}]_{i,j} \cdot [A_2 \nabla z_{i,k,1} + \cdots$$

$$+A_9 \nabla z_{i,k,8}] \quad (3.10)$$

where $\nabla z_{i,k,1} = (\frac{\Delta z}{\Delta s})_{i,k,1} = (\frac{z_2 - z_1}{\Delta s})_{i,k,1}$ computed for distance category, 1, from Table 4, Δs is distance along the wind direction i and is positive downwind.

$(|\vec{\bar{V}}|_{700})_{i,j}$ = class-interval mid-point speed of 24 hour mean Grand Junction 700 mb wind in class i, j (common to all stations and slopes in a given i,j category).

$[(\overline{\frac{\partial qs}{\partial z}})_{700}]_{i,j}$ = mean local vertical change of Grand Junction 700 mb saturation mixing ratio derived from assuming a saturated air mass rising moist adiabatically. Values were estimated using finite increments of Δz about

TABLE 6

Example of Input Data for One Regression Analysis. $B_{i,j} = [(\frac{\partial \overline{qs}}{\partial z})_{700}]_{i,j} \cdot (|\overline{\vec{\nabla}}|_{700})_{i,j}$. Sample Size 15

Dependent Variables	Independent Variables				
	Station Elevation	Station Slope Variables			
$(\overline{R}_t)_{i,j,1}$	z_1	$B_{i,j}\nabla z_{i,1,1}$	$B_{i,j}\nabla z_{i,1,2}$	...	$B_{i,j}\nabla z_{i,1,8}$
$(\overline{R}_t)_{i,j,2}$	z_2	$B_{i,j}\nabla z_{i,2,1}$	$B_{i,j}\nabla z_{i,2,2}$	...	$B_{i,j}\nabla z_{i,2,8}$
o	o	o	o		o
o	o	o	o		o
o	o	o	o		o
$(\overline{R}_t)_{i,j,15}$	z_{15}	$B_{i,j}\nabla z_{i,15,1}$	$B_{i,j}\nabla z_{i,15,2}$	...	$B_{i,j}\nabla z_{i,15,8}$

the 700 mb level from a Stüve diagram. They are listed in units of g kg^{-1} km^{-1} in Table 3.

For this part of the study only direction class i = 1, . . .,7 (see Table 3) were used, as sample sizes of "precipitation days" were insufficient for stability in the precipitation averages in the other categories. Also, five of the original precipitation stations were eliminated on the basis of period of record, or in the case of Wolf Creek Pass, a change in the time of day for measurement. The records of the remaining 15 stations listed in the left-hand column of Table 1 were used in the regression analyses. Results are discussed in Section 4.2.

3.5.3 Testing the Results

The seasons for 1967-68 and 1968-69 were used to test the predictive ability of the resulting regression equations from Section 3.5.2. Computations of calculated versus observed precipitation values were made for each station k in each i,j category using various equation sets from Section 3.5.2. Single regression analysis was performed between observed and calculated values. Results are discussed in Section 4.3.

Also, in order to determine the validity of the methods for computing the terrain slope factors and assessing their importance in explaining precipitation, terrain slope and elevation factors were computed for two points, each only 5 km removed from Silverton (Figure 2). Precipitation values calculated from the various regression equations derived by Section 3.5.2 were obtained using these terrain factors as input and were compared to observed values at Silverton.

Finally, it would be highly desirable to be able to use the regression equations in other areas. To test their applicability in another mountainous region of Colorado where the Grand Junction 700 mb data is still reasonably valid, Steamboat Springs was selected as a test case and treated similarly to the two test points near Silverton. (See Figure 3).

3.5.4 Other Tentative Investigations

The major study was designed to determine the feasibility of explaining observed precipitation at a point on the basis of only some of the orographic and thermodynamic factors in Equation (3.7). Specifically, it ignores dependence on moist air pressure depth and duration of precipitation. Brief consideration is given to these variables in Section 4.4.

Also, as pointed out in Sections 1.2 and 3.1, substantial precipitation is derived from large scale convergence. Through the divergence and absolute vorticity theorems, large-scale convergence precipitation should be proportional to the time rate of change of vorticity, $\dot{\zeta}$. This fact is briefly studied in relation to estimated non-orographic precipitation values in Section 4.4.

4.0 RESULTS AND INTERPRETATION

4.1 Normalized Precipitation Maps

Examples of the set of maps of normalized precipitation values derived according to 3.5.1 are shown in Figures 6 through 9.

Contouring was done according to station ratio values and also purposely considered major barrier orientation. (That is, barrier orientation and location effects as exemplified by ratio values at existing stations were extrapolated or interpolated into silent areas using topographic similarity as a guideline).

The map set reveals two scales of topographic effect. First the upslope and downslope effects of the overall San Juan Mountain massif are plainly evident. Also, more localized effects can be seen at most stations where attention is focused on the topography around a particular location.

These results must be viewed only qualitatively, however, due to the nature in which the contours were drawn and from the lack of numerical values of topographic factors.

4.2 Statistical Treatment

It would be highly desirable to obtain a regression equation explaining virtually all of the precipitation variance and which would be valid for all locations, speeds, directions, and temperatures. Realistically, though, there are numerous complicating factors working to prevent this accomplishment. These include:

(1) An expected systematic change in mean cloud depth and $\frac{\partial qs}{\partial z}$ (due to $\overline{T}$ change) with wind direction due to differing large scale vertical motion fields in selective

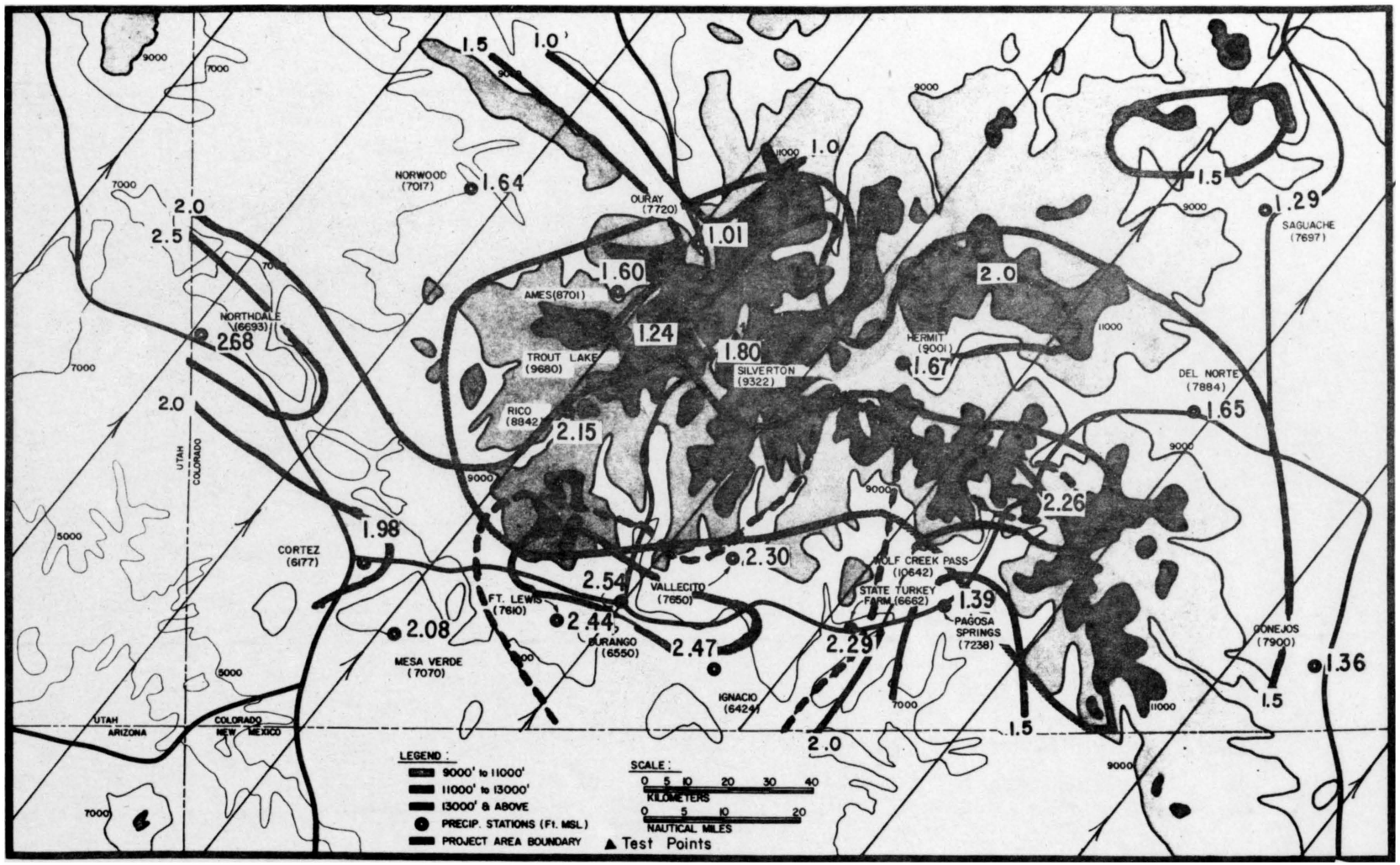

Figure 6. Pattern of $(\bar{R}_t)_{2,k}/(\bar{R}_t)_k$ for 700mb wind direction category 2 (205°-234°). Arrows indicate flow along center direction of wind category (E.G.&G., 1970).

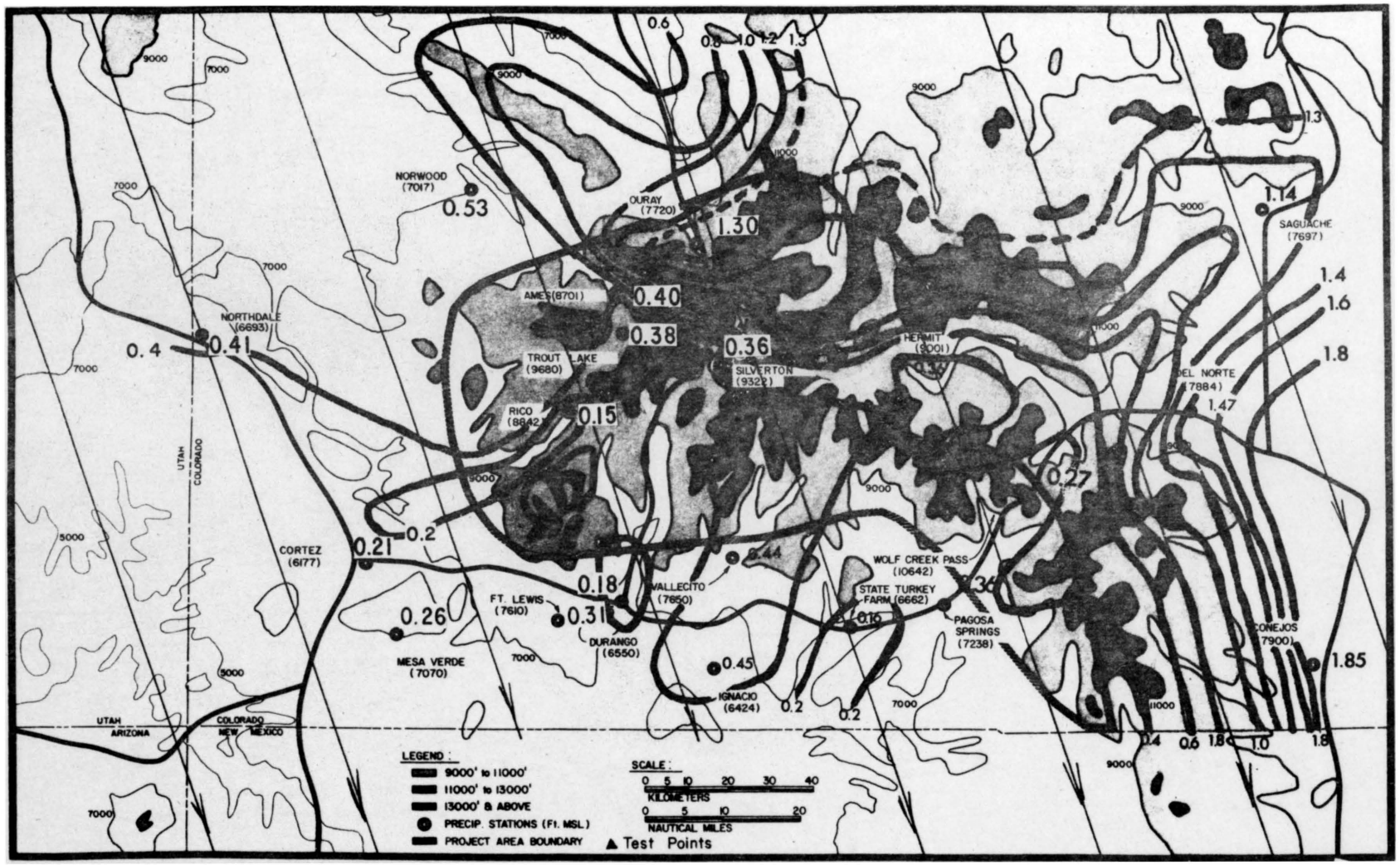

Figure 7. Pattern of $(\bar{R}_t)_{6,k}/(\bar{R}_t)_k$ for 700mb wind direction category 6 (325°-354°). Arrows indicate flow along center direction of wind category (E.G.&G., 1970).

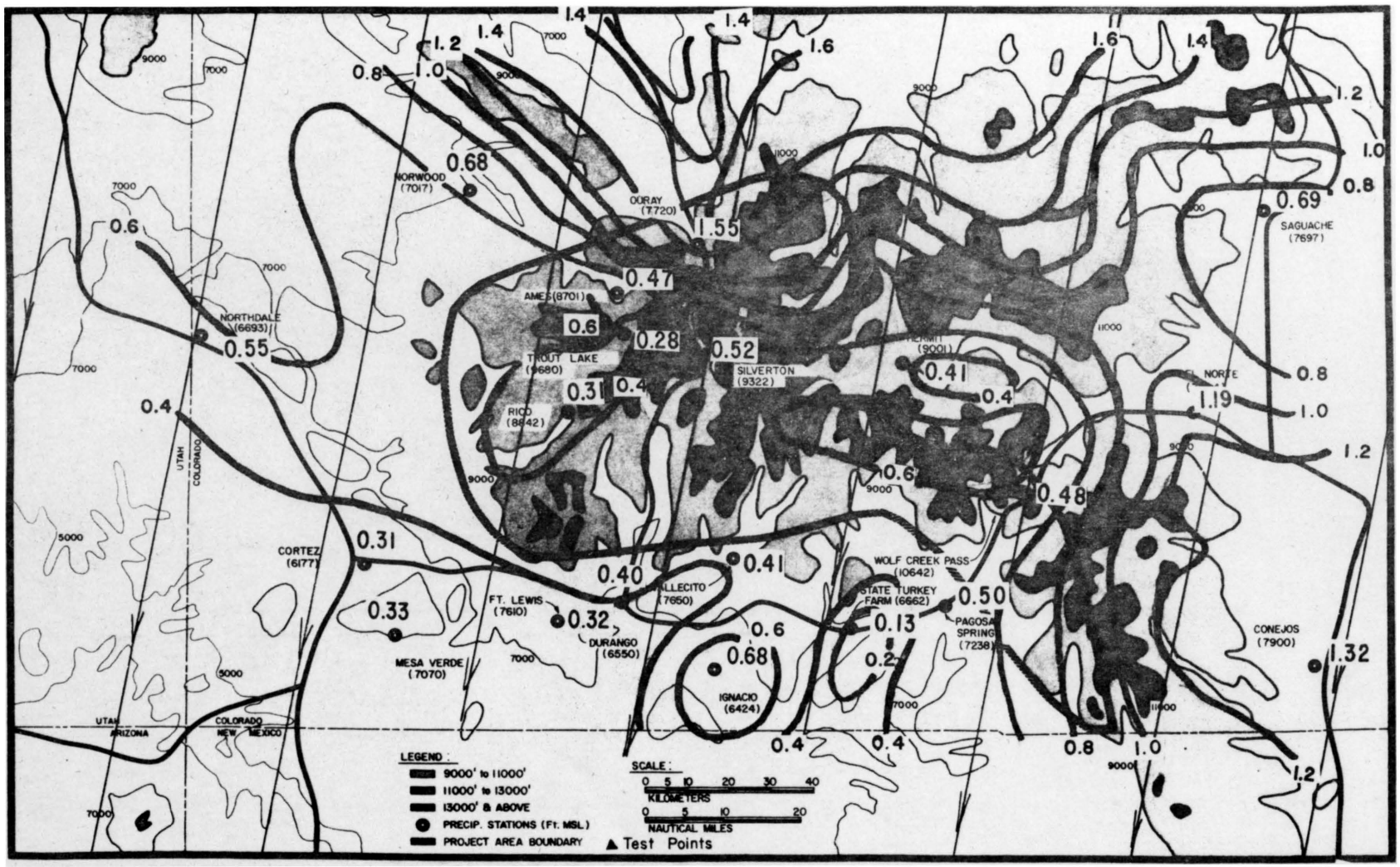

Figure 8. Pattern of $(\bar{R}_t)_{7,k}/(\bar{R}_t)_k$ for 700mb wind direction category 7 (355°-024°). Arrows indicate flow along center direction of wind category (E.G.&G., 1970).

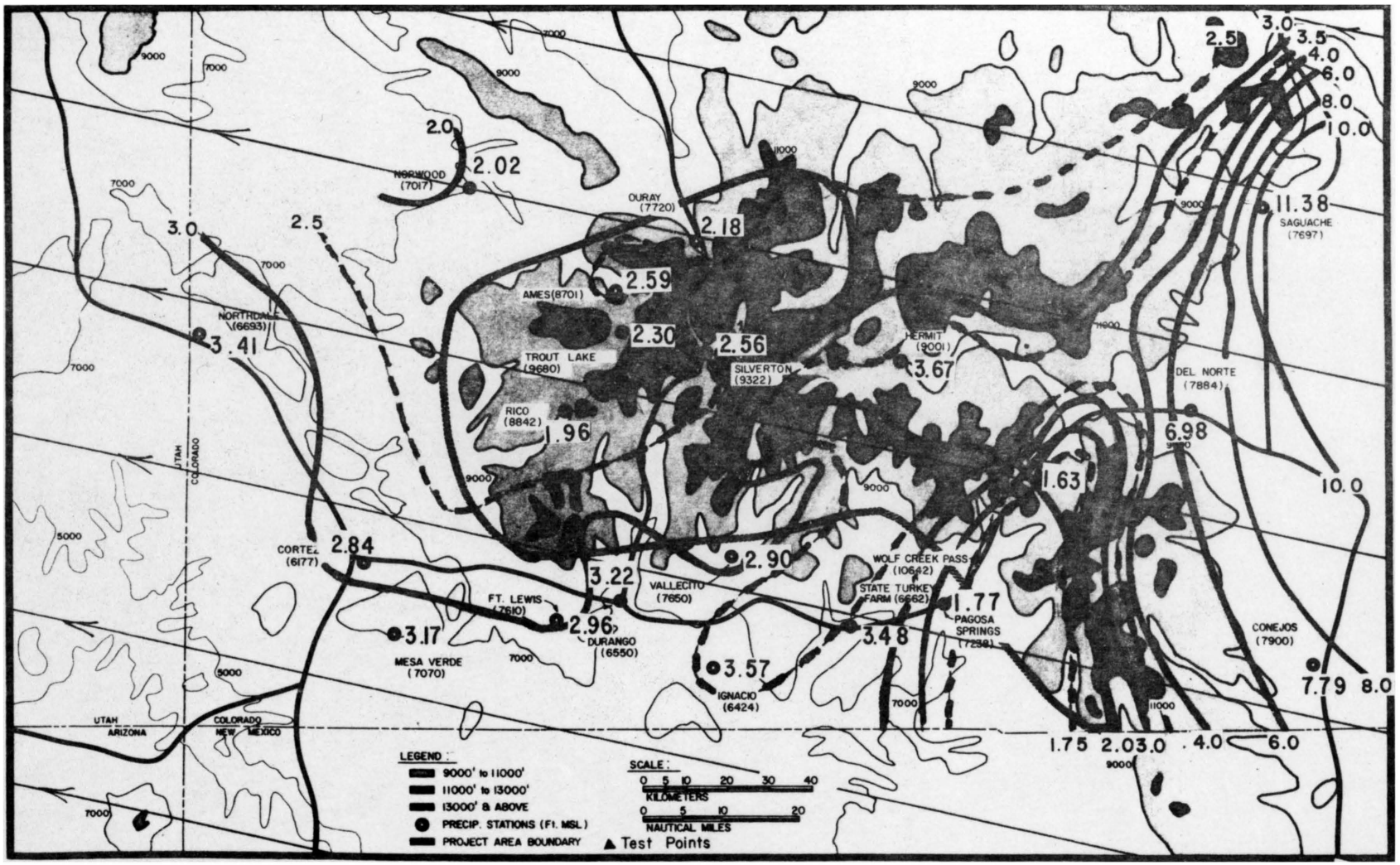

Figure 9. Pattern of $(\bar{R}_t)_{10,k}/(\bar{R}_t)_k$ for 700mb wind direction category 10 (085°-114°). Arrows indicate flow along center direction of wind category (E.G.&G., 1970).

regions of migratory waves (decreasing vertical motion with veering wind).

(2) Corresponding systematic change in the magnitude of non-orographic precipitation components, R_d and R_c (decreasing magnitude as the wind veers).

(3) Highly complex effects on snow crystal trajectories as temperature, $\overline{T}$ changes.

(4) Marked changes in snow crystal trajectories with wind speed variations.

(5) Local topographic pecularities unique to each station.

Therefore, the highest correlation is to be expected by minimizing as many of these factors as possible.

In the discussions of regression analysis results that follow reference is frequently made to the above five (5) complicating factors and also to Table 5 from Section 3.5. In fact the following sub-section titles are identical to the stratification descriptions in corresponding Sections of Table 5. Also, since the number of pages of tables and figures considerably exceed the pages of text, grouped stacking of text, tables and figures (in that order) is observed for the next two major sub-sections in Section 4 (i.e., for Section 4.2 and 4.3).

4.2.1 Speed and Direction Constant

Factors (1) through (4) above, can be held constant by restricting the regression analysis to the precipitation and terrain data set for a given direction (i) and speed (j) category. This was done for each of the 27 combinations of i,j Table 3, and 27 uniquely different regression equations were obtained. Sample size in each analysis was 15 (because there are 15 precipitation stations). Multiple

correlation coefficients were quite high (0.8 to 0.98). The complete set of multiple and single correlation coefficients is presented in Table 7.

Regression equation coefficients are correspondingly displayed in Table 8. These equations calculate 24 hour precipitation in inches when (1) station elevation is given in meters and (2) $(\overline{\frac{\partial qs}{\partial z}})_{700}$ is given in g kg^{-1} km^{-1}, 700 mb 24 hour mean wind speed, j, is in m sec^{-1} and terrain slopes are dimensionless and computed for the distances shown in Table 4.

Interesting features observable from Table 7 and Table 8 include:

(1) a generally high single correlation between precipitation and the terrain slopes computed over the distances 10 km downwind to 20 km upwind ($\nabla z_{i,k,3}$) and also 40 km either direction from the station ($\nabla z_{i,k,1}$)

(2) occasional systematic increase in the importance of more upstream slope factors as wind speed increases

(3) generally only slight single correlation to station elevation

(4) considerable inconsistency of the signs and magnitudes of the resulting regression equation coefficients

(5) frequent negative single correlation to the slope over the first 10 km upwind of the station ($\nabla z_{i,k,4}$). This is explicable since the stations with heavier precipitation are located locally in deep valleys amidst surrounding high peaks and near the San Juan crest. The stations with lighter average precipitation, on the other hand, are generally farther removed from the San Juan

TABLE 7

Summary Table of Regression Analyses Performed with Direction and Speed Constant

Direction Category i	Speed Category j	Sample Size	Range of $(\bar{R}_t)_{i,j,k}$	Std. Error of Est.	Multiple R	Multiple R^2	Degree of Freedom		F Ratio	Elevation	Single Correlation Coefficients								No. Precip. Days Over Which $(R_t)_{i,j,k}$ Calculated
							Regression	Residual			+40 -40 1	+20 -30 2	+10 -20 3	0 -10 4	0 -30 5	-10 -30 6	-10 -40 7	-10 -50 8	
1	1	15	.06 - .28	.033	.959	.920	8	6	8.59	-.210	.60	.43	.27	.49	.29	-.18	-.33	-.43	18
1	2	15	.05 - .30	.025	.975	.950	9	5	10.59	.066	.80	.68	.83	.56	.56	.08	.35	.35	13
1	4	15	T - .41	.057	.954	.909	9	5	5.57	.212	.68	.75	.79	.30	.46	.26	.41	.40	6
2	1	15	.05 - .34	.026	.971	.943	8	6	12.31	-.005	.46	.73	.39	-.10	.47	.55	.42	.22	17
2	2	15	.08 - .37	.052	.925	.855	9	5	3.28	-.038	.79	.83	.82	.43	.75	.35	.39	.35	35
2	2	15	.03 - .37	.044	.962	.925	8	6	9.25	.103	.78	.78	.62	.10	.56	.54	.61	.42	20
2	4	15	.04 - .61	.112	.914	.836	9	5	2.83	.366	.54	.59	.57	-.03	.42	.48	.58	.41	12
3	1	15	.01 - .18	.032	.832	.693	7	7	2.25	.291	.54	.62	.67	-.37	.25	.67	.65	.66	28
3	2	15	.02 - .19	.025	.935	.873	8	6	5.16	.354	.61	.64	.70	-.38	.34	.78	.78	.83	67
3	3	15	.02 - .25	.029	.963	.927	8	6	9.51	.185	.75	.60	.63	-.19	.37	.59	.59	.69	34
3	4	15	.02 - .30	.050	.906	.820	8	6	3.42	.257	.58	.50	.61	-.22	.29	.54	.46	.58	22
3	5	15	.00 - .48	.109	.844	.713	8	6	1.86	.251	.57	.63	.60	-.26	.34	.64	.60	.68	7
3	6	15	.08 - .82	.196	.840	.706	8	6	1.79	.368	.46	.41	.46	-.22	.21	.47	.39	.50	3
4	1	15	.02 - .13	.029	.823	.677	8	6	1.57	.175	.60	.60	.51	-.51	.20	.67	.60	.44	34
4	2	15	.01 - .11	.010	.982	.963	8	6	19 66	.376	.73	.74	.89	-.42	.47	.85	.85	.74	76
4	3	15	.02 - .15	.013	.978	.956	7	7	21.82	.642	.62	.48	.68	-.53	.22	.71	.77	.64	44
4	4	15	T - .10	.025	.816	.666	7	7	2.00	.484	.41	.43	.55	-.50	.21	.66	.65	.49	9
5	1	15	.02 - .14	.025	.897	.805	7	7	4.11	.535	.69	.68	.71	-.09	.22	.29	.41	.47	27
5	2	15	.01 - .20	.018	.974	.948	8	6	13.66	.396	.72	.76	.84	-.16	.22	.34	.44	.44	41
5	3	15	01 - .10	.015	.945	.894	8	6	6.30	.645	.51	.67	.65	-.51	.15	.50	.60	.62	20
5	4	15	.00 - .20	.022	.969	.938	8	6	11.34	.720	.44	.63	.57	-.57	.04	.42	.54	.61	7
6	1	15	.01 - .12	.018	.917	.841	8	6	3.97	.184	.68	.63	.74	-.05	.35	.33	.37	.46	20
6	2	15	T - .17	.026	.900	.809	8	6	3.18	.259	.60	.58	.65	-.15	.19	.27	.31	.43	25
6	3	15	.00 - .20	.065	.843	.711	7	7	2.45	.366	.60	.62	.57	-.18	.22	.32	.35	.52	4
7	1	15	.01 - .12	.026	.788	.620	8	6	1.23	.283	.45	.43	.36	-.49	-.01	.24	.33	.38	18
7	2	15	T - .16	.029	.883	.780	8	6	2.66	.133	.58	.47	.60	-.49	.05	.20	.41	.49	19
7	3	15	0 - .2	.039	.877	.769	8	6	2.50	.143	.53	.39	.47	-.32	-.08	.11	.34	.46	4

TABLE 8

Regression Equation Coefficients for Speed and Direction Constant

Direction	Speed	Constant	Elev.	1	2	3	4	5	6	7	8
1	1	-.13749	.00013	2.29357	-.49686	.00000	-.63756	1.61525	-.80593	-1.22005	-.30981
	2	.04905	.00004	.92389	-.43766	.37813	-.17225	.39887	-.23522	-.94204	.95863
	4	-.05690	.00009	.67856	-.22899	.49761	-.25646	.34868	-.21576	-.51726	.25607
2	1	-.12887	.00010	.00000	1.87013	-.24675	-.27638	.61375	-.29819	-.76802	-.19816
	2	.11968	.00002	.11732	.63104	.41385	-.04333	-.11313	.05530	-.41172	-.17505
	3	-.44067	.00024	.90888	.38608	-.51613	-.06794	.34924	-.16027	.00000	.09897
	4	-1.25358	.00063	.41846	.63990	-.62450	-.18732	1.02689	-.71895	.30322	.30677
3	1	-.02494	.00004	.54285	.06999	.16869	0.03722	.00000	.15931	.00000	-.29357
	2	-.08723	.00007	.36168	-.03641	-.06760	.03602	.00000	.25552	-.10378	.06105
	3	-.16532	.00011	.87391	-.10023	-.19369	.00000	.09664	.36999	-.55619	.18919
	4	-.11478	.00010	.61145	-.24635	.07141	-.00543	.00000	.32052	-.58161	.28254
	5	-.39100	.00022	.54818	.14253	-.26942	.05356	.00000	.33224	-.34033	.21487
	6	-.91304	.00051	1.44842	-.35748	-.39295	.08399	.00000	.97964	-1.16224	.28898
4	1	.09740	-.00002	.29939	.00000	.06870	-2.58946	7.60135	-4.85245	-.57790	.48999
	2	.02208	.00002	-.01818	.05917	.12776	.00000	.03140	.04498	.12018	-.08934
	3	-.14333	.00009	-.24862	.00000	.04714	-.07434	.25231	.00000	-.06354	.27857
	4	-.03002	.00004	-.04339	.00000	.01126	.00000	.01503	.06225	.06356	-.06323
5	1	-.08399	.00005	.96737	-.45739	.20545	-.03953	-.21863	.00000	.00000	-.02082
	2	.02059	.00000	.41132	-.06941	.23268	-.01763	-.35050	.00000	.25881	-.20696
	3	0.02260	.00002	.02907	.05300	.04920	-.02542	-.09167	.00000	.08603	-.03203
	4	-.08506	.00004	-.07140	.18912	.04792	-.02060	-.18512	.00000	.12715	-.00855
6	1	.14174	-.00006	-.12786	.02205	.34043	-.02120	-.47065	.00000	.07617	.32382
	2	.18896	-.00008	-.13837	.13394	.22837	-.16729	.00000	-.33485	.04557	.30600
	3	.21614	-.00008	.42255	.21974	.05245	.00000	-.53769	.00000	-.19271	.52943
7	1	.18001	-.00008	-.10231	.68675	-.24826	-.21315	.00000	-.29150	.10861	.08418
	2	22849	-.00011	-.24330	.31137	.02283	.00000	-.39298	-.11454	.35893	.15733
	3	.42285	-.00017	1.62817	-1.03689	.23768	-.55373	.95312	.00000	-1.24224	.61725

crest and are not in such deep local valleys. Therefore, $\nabla z_{i,k,4}$ values are not as negatively large.

4.2.2 Wind Direction Constant; Speed Variable

Referring to the stated complicating factors in Section 4.2, variations in cloud depth and non-orographic precipitation (factors (1) and (2), respectively) can be minimized by keeping only wind direction class, i, constant. By allowing wind speed class to vary the wind factor, (4), can be expected to induce complications and to the extent mean temperature, $\bar{T}$, changes, so will factor (3).

To test the severity of effect of these complications regression analysis was made for each of the 7 sets of precipitation data obtainable from Table 3 when classifying separately only by wind direction category, i. Sample sizes for each analysis were 45 for i = 1, 6 and 7, 60 for i = 2, 4 and 5, and 90 for i = 3.

The resulting set of seven (7) regression analyses (one for each direction class, i) still showed fairly high multiple correlation coefficients (0.74 to 0.85).

4.2.3 Direction, Speed and Temperature Variable

As discussed in the introductory remarks of Section 4.2, it would be desirable to obtain one general valid regression equation applicable for all points, speeds, directions and temperatures. This section attempted such an accomplishment even though the chances for success (high correlation) were not high.

The procedure was to run a regression analysis on the entire data sample of size 405 (i.e., the sample resulting from 27 combinations of i,j classes, each containing 15 $(\bar{R}_t)_{i,j,k}$ from Table 3.

The resulting lower multiple correlation coefficient of 0.69 reflects the existence of the expected effect of giving free range to all five (5) complicating factors as listed in Section 4.2.

4.2.4 Direction, Speed and Temperature Variable Non-Orographic Components Isolated

The analysis to obtain one general regression equation in the preceeding section made no attempt at isolating $(\bar{R}_o)_{i,j,k}$ from $(\bar{R}_d + \bar{R}_c)_{i,j,k}$. Rather, it gave free range to all the complicating factors listed in Section 4.2 and the resulting correlation was only modest (0.69). If $(\bar{R}_t)_{i,j,k}$ could be divided into $\bar{R}_o$ and $\bar{R}_d + \bar{R}_c$ components, a more valid general regression equation might be obtainable by considering only $(\bar{R}_o)_{i,j,k}$ in relation to terrain variables.

This was attempted in an early part of the study in the manner discribed below. The procedure was then extended to the larger data set.

In an early part of the study regression analysis was performed on the data set consisting of mean precipitation values derived from pooling wind speed categories 2 and 3 (13-18 and 19-24 kts) together as one class. Resulting multiple correlation was again very high as was single correlation to the +10 to -20 km slope value ($\nabla z_{i,k,3}$ from Table 4). When plotting actual station precipitation against this slope for a given direction category, two interesting observations could be made (from examples in Figure 10). First, the slope of the visual best fit regression line decreased systematically with more westerly or northerly direction categories (i.e., the inter-station range of $(\bar{R}_t)_{i,j,k}$ decreased). Secondly, the estimated precipitation value (visual regression line value) for the point of zero terrain slope ($\nabla z_{i,k,3}=0$) decreased systematically for veering wind direction categories.

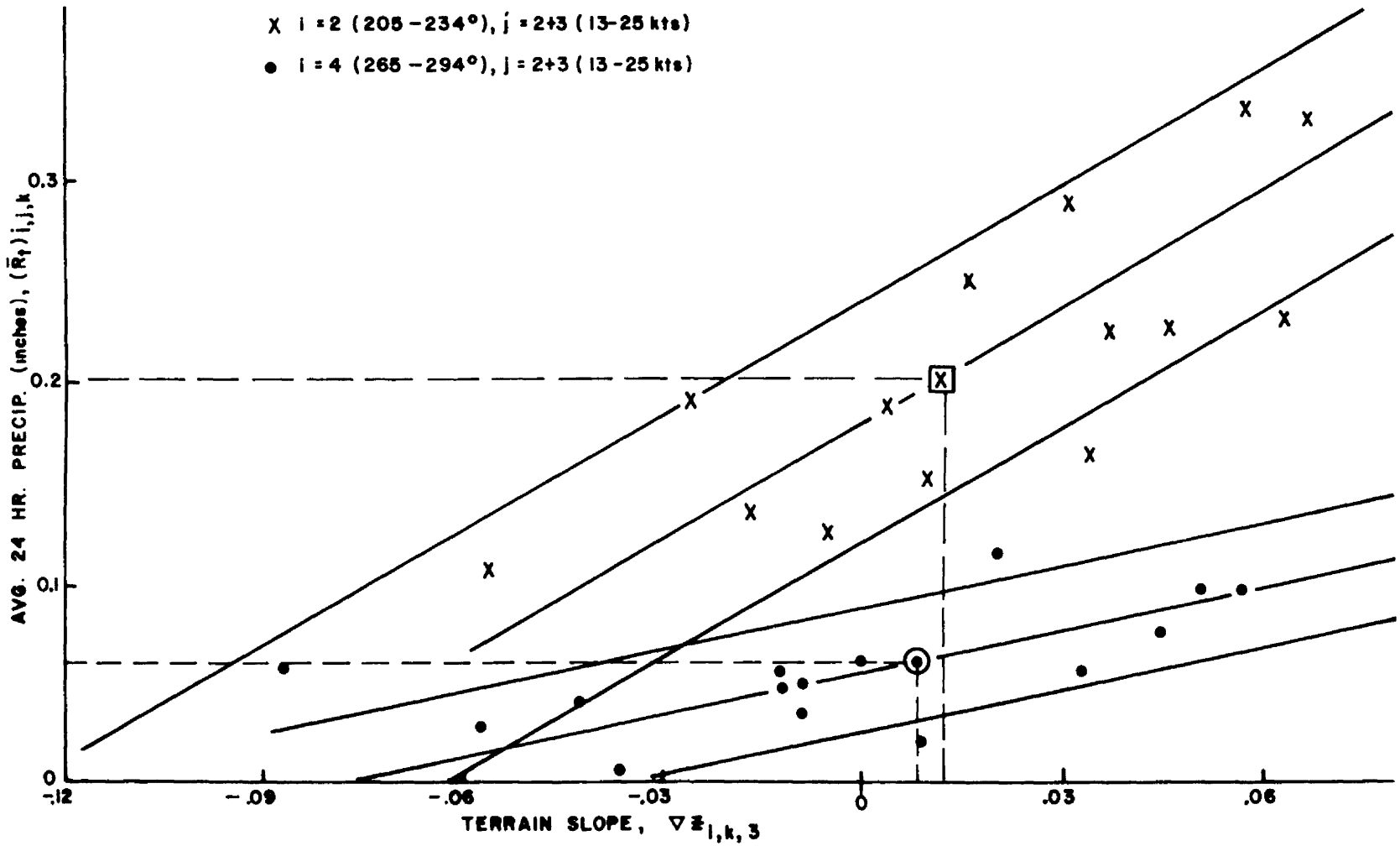

Figure 10. Selected scatter plots of $(R_t)_{i,j,k}$ vs. terrain slope, $\nabla z_{i,k,3}$. Rough estimates of lines of best fit and standard error limits are shown.

This value of precipitation at zero terrain slope was taken to be the non-orographic component $(R_d + R_c)_{i,j,k}$ for a given direction category, and was assumed to be affecting all stations equally. It was consequently subtracted from each value of the appropriate set of data and the resulting entire sample of 105 cases (15 stations and 7 directions) was input to the regression analysis program. A multiple correlation coefficient of 0.79 was obtained therefrom.

This same technique was used on the set of 405 cases (as in Section 4.2.3) by substituting estimated $(\bar{R}_o)_{i,j,k}$ for $(\bar{R}_t)_{i,j,k}$ where

$$(\bar{R}_o)_{i,j,k} = (\bar{R}_t)_{i,j,k} - \text{EST. } (\bar{R}_d+\bar{R}_c)_{i,j,k} \qquad (4.1)$$

and values of EST. $(\bar{R}_d+\bar{R}_c)_{i,j,k}$ were obtained from the appropriate direction categories from the above described early part of the study. The resulting correlation coefficient from the multiple regression analysis was only 0.71. Thus, only slight improvement was obtained compared to the 0.69 r-value found in Section 4.2.3.

4.2.5 Direction, Speed, and Temperature Variable; Station Constant

The effect of local station topographic peculiarities (factor (5) in Section 4.2) was minimized at the expense of giving free range to all other complications ((1) through (4) of Section 4.2) and regression equations were computed for each station by allowing wind and temperature to vary. Sample size in each case was 27 (because of the 27 i, j joint classes).

Table 9 lists pertinent correlation results and standard errors of estimates (see Table 1 for station number key). Voluminous interpretative (or speculative) comments could be made in relation to station terrain profiles. However, since the most important testing

TABLE 9

Summary Table of Regression Analyses Performed with
Direction, Speed, and Temperature Variable, Station Constant

Station	Sample Size		Std. Error of Est.	Multiple R	Multiple R^2	Degree of Freedom		F Ratio	Elevation	Single Correlation Coefficients							
						Regression	Residual			1	2	3	4	5	6	7	8
1	27		.068	.898	.807	7	19	11.31	-.001	.168	-.087	-.504	-.870	-.715	.771	.736	.466
2	27		.027	.902	.813	7	19	11.79	-.000	.072	.368	.072	.068	.340	.000	.761	.688
3	27		.056	.513	.263	7	19	.97	-.000	.078	-.076	.078	-.076	.143	.191	.241	.260
4	27		.066	.917	.840	6	20	17.51	.000	.883	.850	.722	.037	.658	.785	.718	.636
5	27		.056	.919	.844	7	19	14.67	.000	.851	.762	.804	.804	.767	.568	.602	.724
6	27		.043	.853	.727	7	19	7.22	-.001	.720	-.070	.047	-.761	-.100	-.393	.548	.438
7	27		.042	.878	.771	6	20	11.21	-.000	.865	.863	.659	-.611	.718	.860	.838	.824
8	27		.042	.926	.858	6	20	20.17	.000	.833	.736	.730	.856	.755	.381	.416	.472
9	27		.035	.902	.814	7	19	11.89	-.001	.433	.767	.820	.562	.820	.562	.338	.361
10	27		.036	.677	.459	6	20	2.82	-.000	-.375	-.126	-.250	-.311	-.207	-.005	.490	.308
11	27		.043	.690	.477	6	20	3.04	.000	.117	.075	.184	.190	.091	-.204	-.148	-.082
12	27		.063	.922	.850	7	19	15.36	-.000	.501	.790	.819	.461	.553	.501	.730	.782
13	27		.061	.958	.916	7	18	27.87	-.000	.851	.788	.892	-.669	.278	.537	.856	.812
14	27		.052	.895	.802	7	19	10.97	-.001	.269	.681	.252	-.068	-.470	.262	.117	.151
15	27		.095	.902	.813	7	19	11.83	.000	.796	.839	.781	.444	.770	.603	.682	.786

of the study is yet to be made in Section 4.3, only the following brief discussions will be presented:

(1) The lowest correlation for Del Norte is to be expected since it is downslope from all direction categories except 7. Therefore, the great majority of individual "precipitation days" (as defined in Section 3.4) from which its $(\bar{R}_t)_{i,j,k}$ were calculated were zero values. Yet the site is within occasional "spill-over" range for snow crystals born over the upwind slopes of the San Juans and borne onto the lee-side by strong south to south-westerly winds.

(2) Ouray is definitely in a complex "spill-over" locality which partially explains the relatively low correlation.

(3) Mesa Verde, Ft. Lewis and Northdale are essentially non-valley stations. Thus, the true importance of representative slope in the first few kilometers upwind is revealed by the high single correlation coefficient to $\nabla z_{i,j,4}$. This contrasts markedly with the strange-looking negative correlation to similar slope factors for many of the other stations. Thus, rather than actual station elevation, a mean over a 5 km radius circle might have been a better choice to minimize the valley location problem.

(4) It is interesting to note from Figure 11 that Silverton (a) is upslope for longer waves (+40 to -40 km; $\nabla z_{i,k,1}$) for all directions but (b) downslope over the 0-10 km range, ($\nabla z_{i,k,4}$) in all directions and (c) average precipitation is relatively low for Silverton. This implies that either (a) there must be very strong evaporation of crystals in the close-in downslope flow or (b) the majority of snow gets physically intercepted by windward slopes of the surrounding barriers.

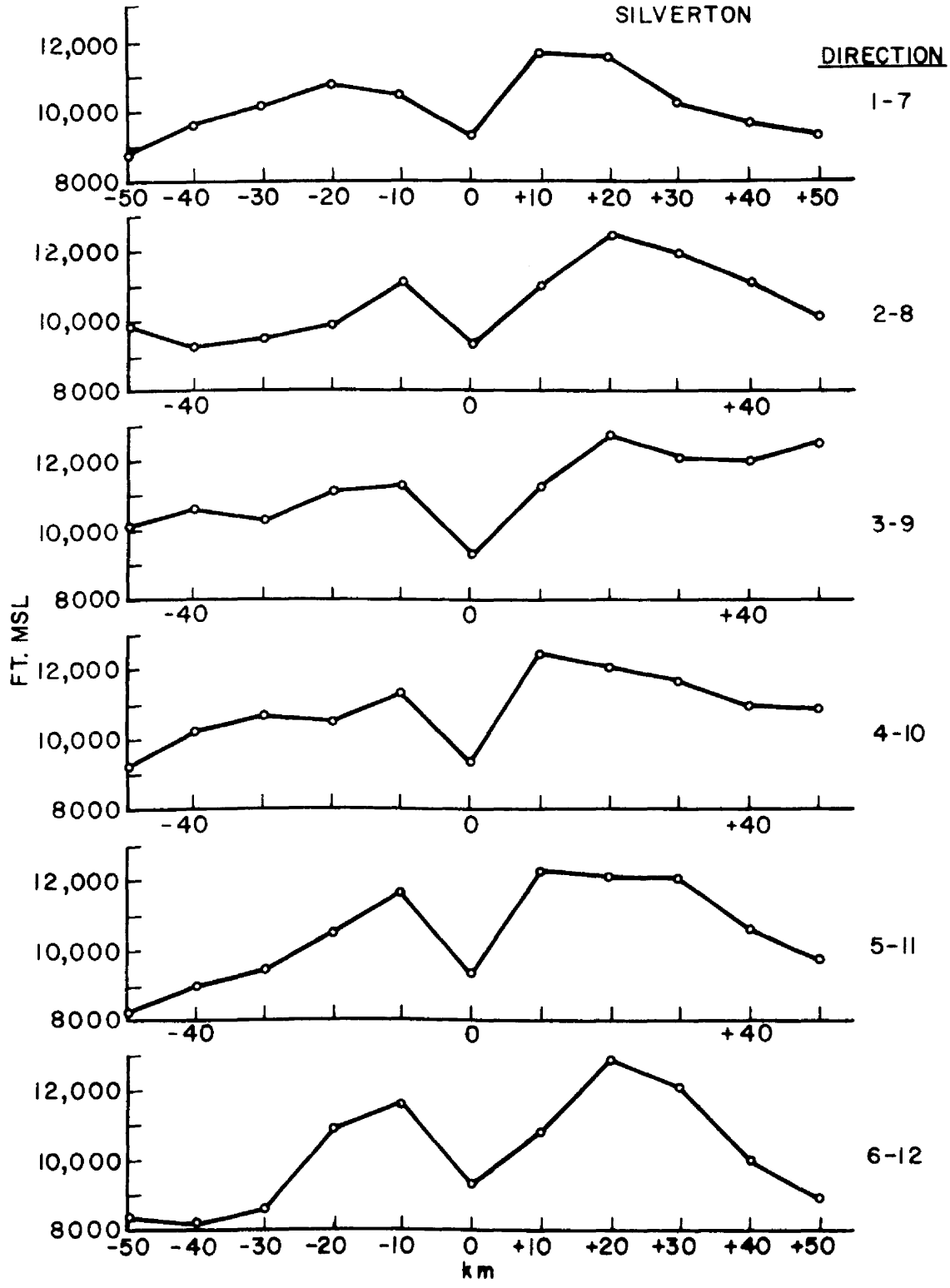

Figure 11. Average terrain profile encountered by air moving over Silverton from left to right (right to left) for direction categories i=1, ..., 6 (7-12) (E.G.&G., 1970).

4.3 Testing the Results

4.3.1 Test Seasons of 1967-68 and 1968-69

The generally very high multiple correlation coefficients obtained in Section 4.2.1 and 4.2.5 are quite encouraging. However, the utility of the derived regression equations for generally specifying mean precipitation at a point can best be verified by comparing calculated to observed values using true test precipitation data. For this purpose, precipitation data was tabulated for two test seasons (1967-68 and 1968-69).

The sets of regression equations from Sections 4.2.1 (Speed and Direction Constant) and 4.2.5 (Station Constant) were used to compute expected values of total precipitation for each station, both for each speed and direction category and also summed over the season. Single regression analysis was performed for each resulting set of calculations. Visual examples of the degree of fit for the seasonal totals are shown in Figures 12 and 13, while examples of individual speed and direction categories are shown in Figures 14-17. The alphabetic characters in these Figures refer to specific precipitation stations. The locator map is given in Figure 18.

As can be observed both from the tables and figures, the correlation of observed to predicted is quite high in most cases where sample size permitted (see also Figure 19) although the observed values were frequently consistently above or below the predicted. That is, there was good inter-correlation of relative precipitation values among stations where even fairly small samples were composited to obtain a total. This implies the general validity of extending the regression equation to predict non-historical data, but cautions that other significant

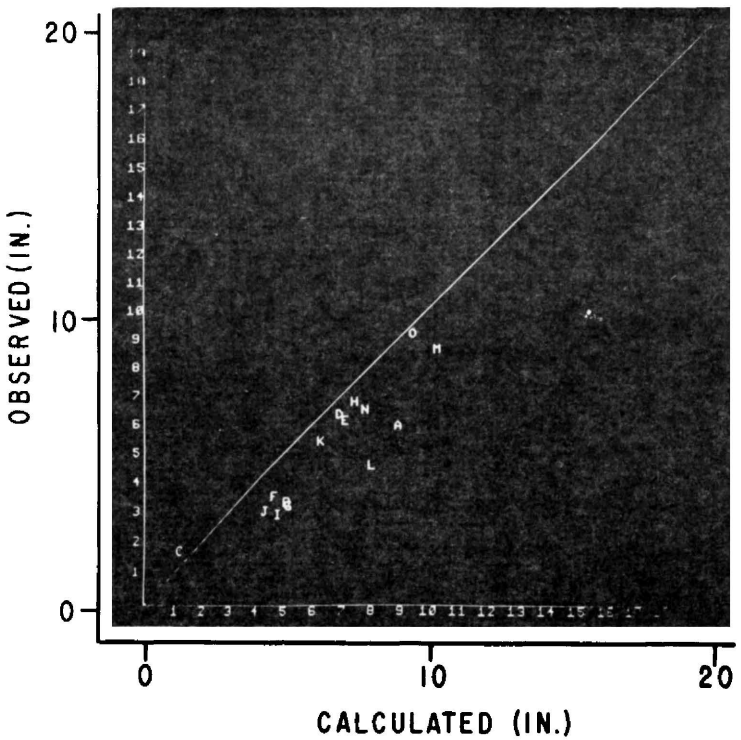

(a)

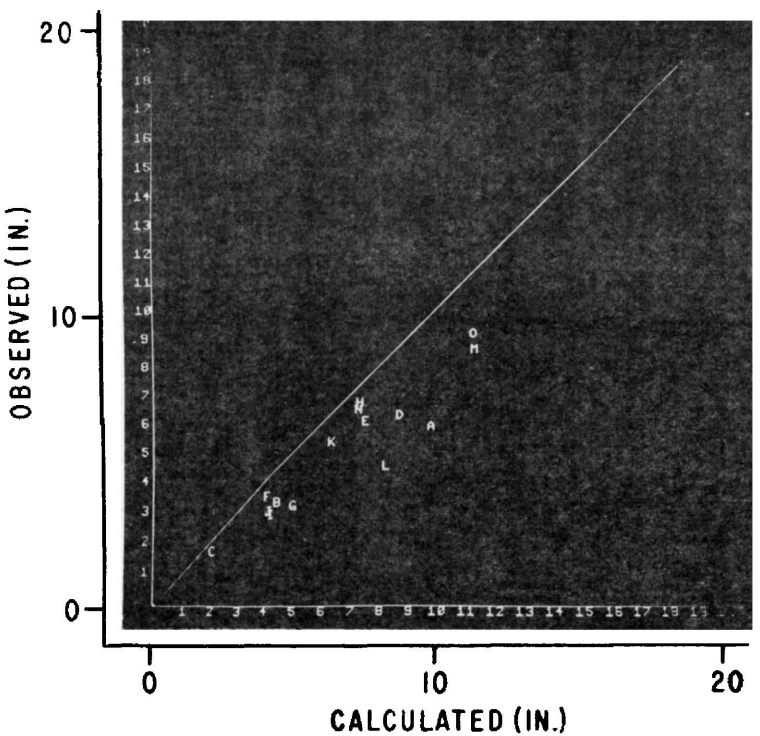

(b)

Figure 12. Scatter plots of computed vs. observed total precipitation for 1967-68 season using regression equations derived from section (a) 4.2.1 and (b) 4.2.5. Alphabetic characters denote specific stations as shown in Figure 41; (r = 0.91 and 0.93 for (a) and (b) respectively).

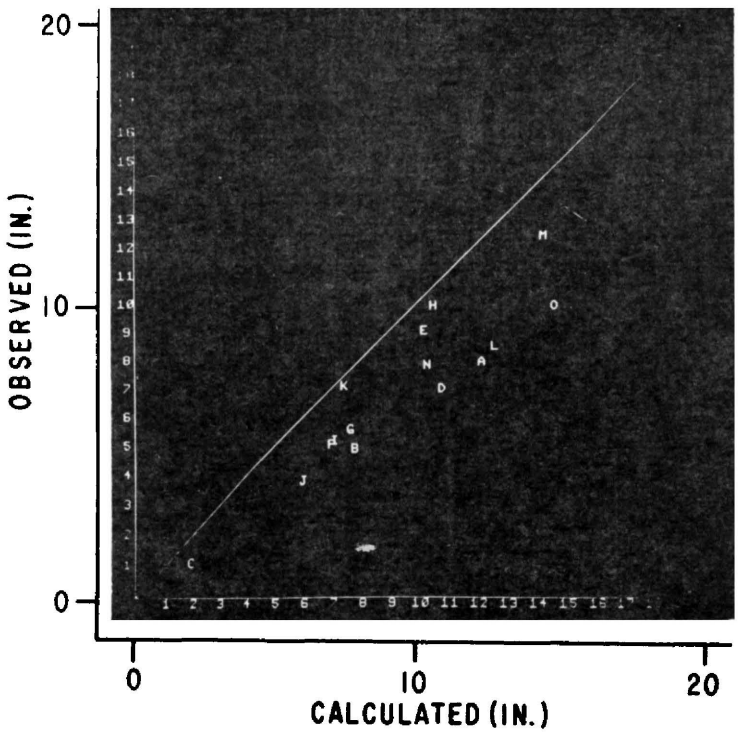

(a)

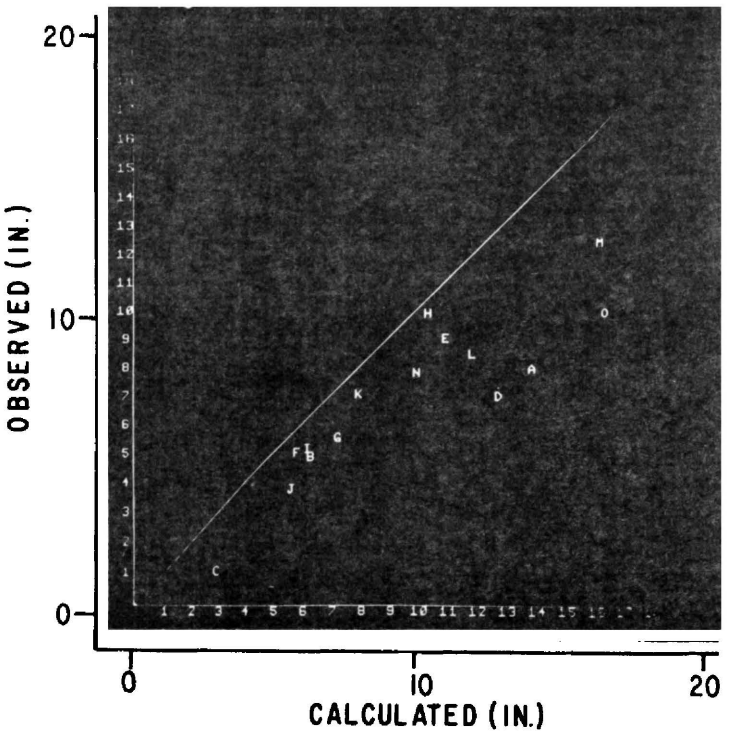

(b)

Figure 13. Scatter plots of computed vs. observed total precipitation for 1968-69 season using regression equations derived from Section (a) 4.2.1 and (b) 4.2.5. Alphabetic characters denote specific stations as shown in Figure 41; (r = 0.92 and 0.89 for (a) and (b), respectively.

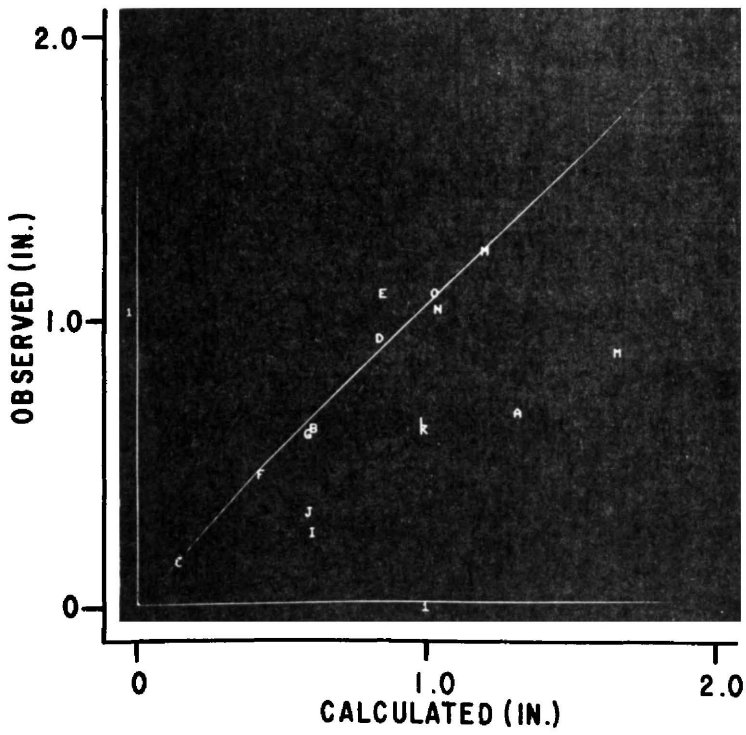

Figure 14. Scatter plot of computed vs. observed $(\overline{R}_t)_{3,2,k}$ for 1967-68. Computed values are from regression equations derived in Section 4.2.2. See Table for correlation coefficients and number of "Precipitation Days" comprising the average $(\overline{R}_t)_{3,2,k}$. Alphabetic characters represent stations (See Figure 41).

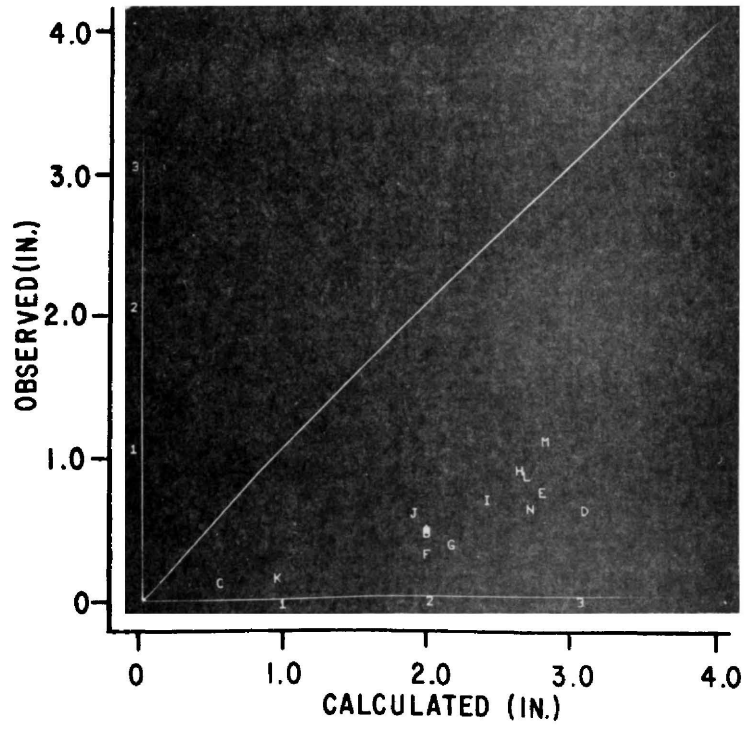

Figure 15. Scatter plot of computed vs. observed $(\overline{R}_t)_{2,2,k}$ for 1968-69. Computed values are from regression equations derived in Section 4.2.2. See Table 14 for correlation coefficients and number of "Precipitation Days" comprising the average $(\overline{R}_t)_{2,2,k}$. Alphabetic characters represent stations (See Figure 41).

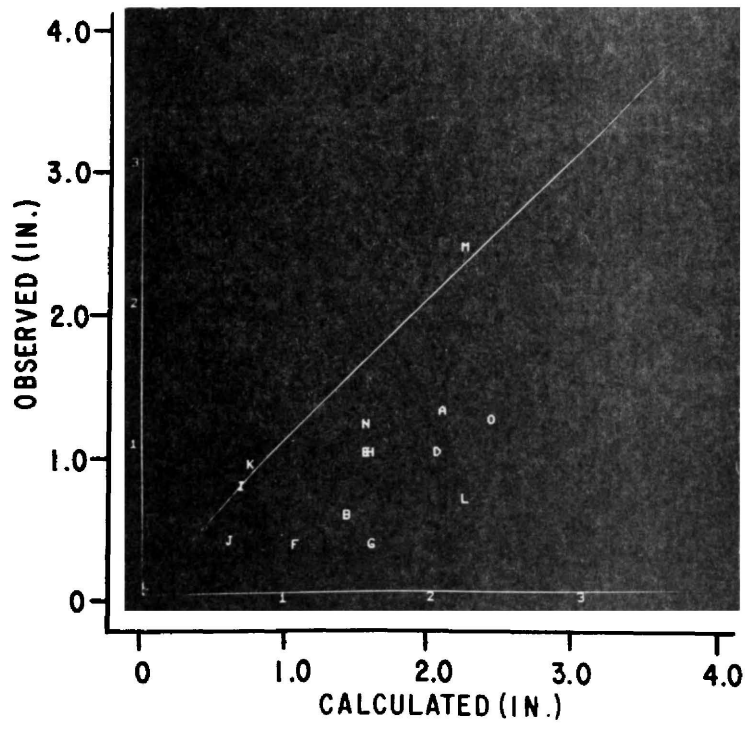

Figure 16. Scatter plot of computed vs. observed $(\overline{R}_t)_{2,3,k}$ for 1968-69. Computed values are from regression equations derived in Section 4.2.2. See Table 14 for correlation coefficients and number of "Precipitation days" comprising the average $(\overline{R}_t)_{2,3,k}$. Alphabetic characters represent stations (See Figure 41).

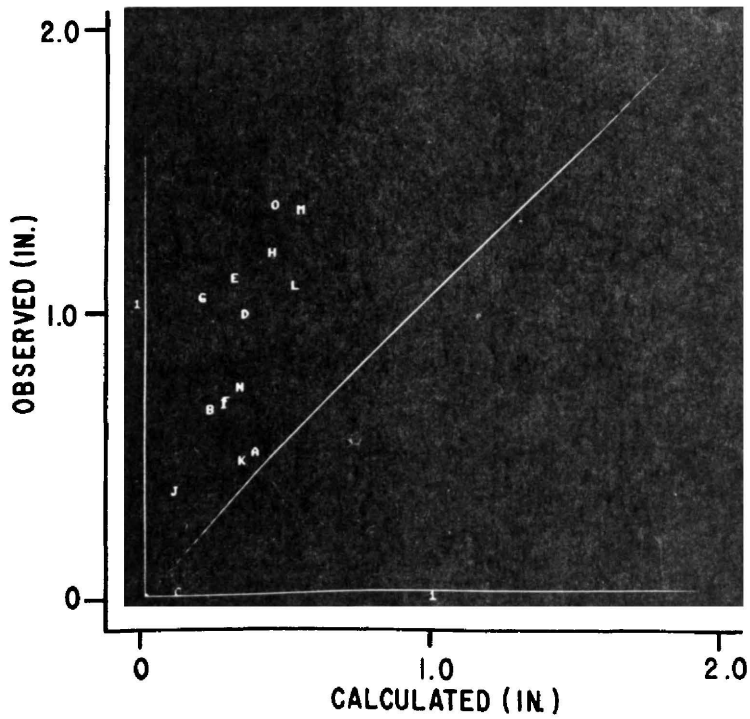

Figure 17. Scatter plot of computed vs. observed $(\overline{R}_t)_{3,4,k}$ for 1968-69. Computed values are from regression equationd derived in Section 4.2.2. See Table 14 for correlation coefficients and number of "Precipitation Days" comprising the average $(\overline{R}_t)_{3,4,k}$. Alphabetic characters represent stations (See Figure 41).

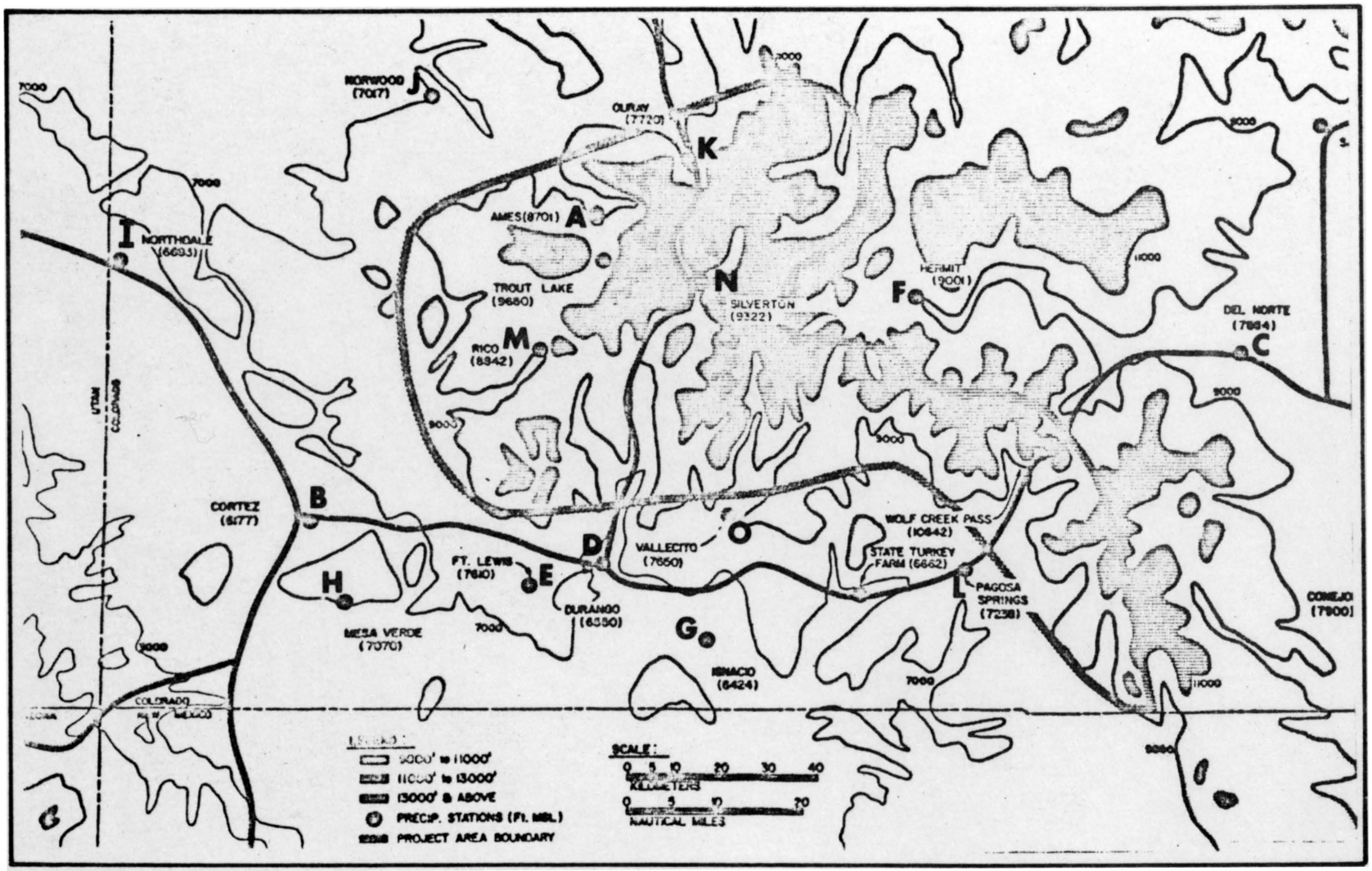

Figure 18. Alphabetic identifiers for precipitation stations.

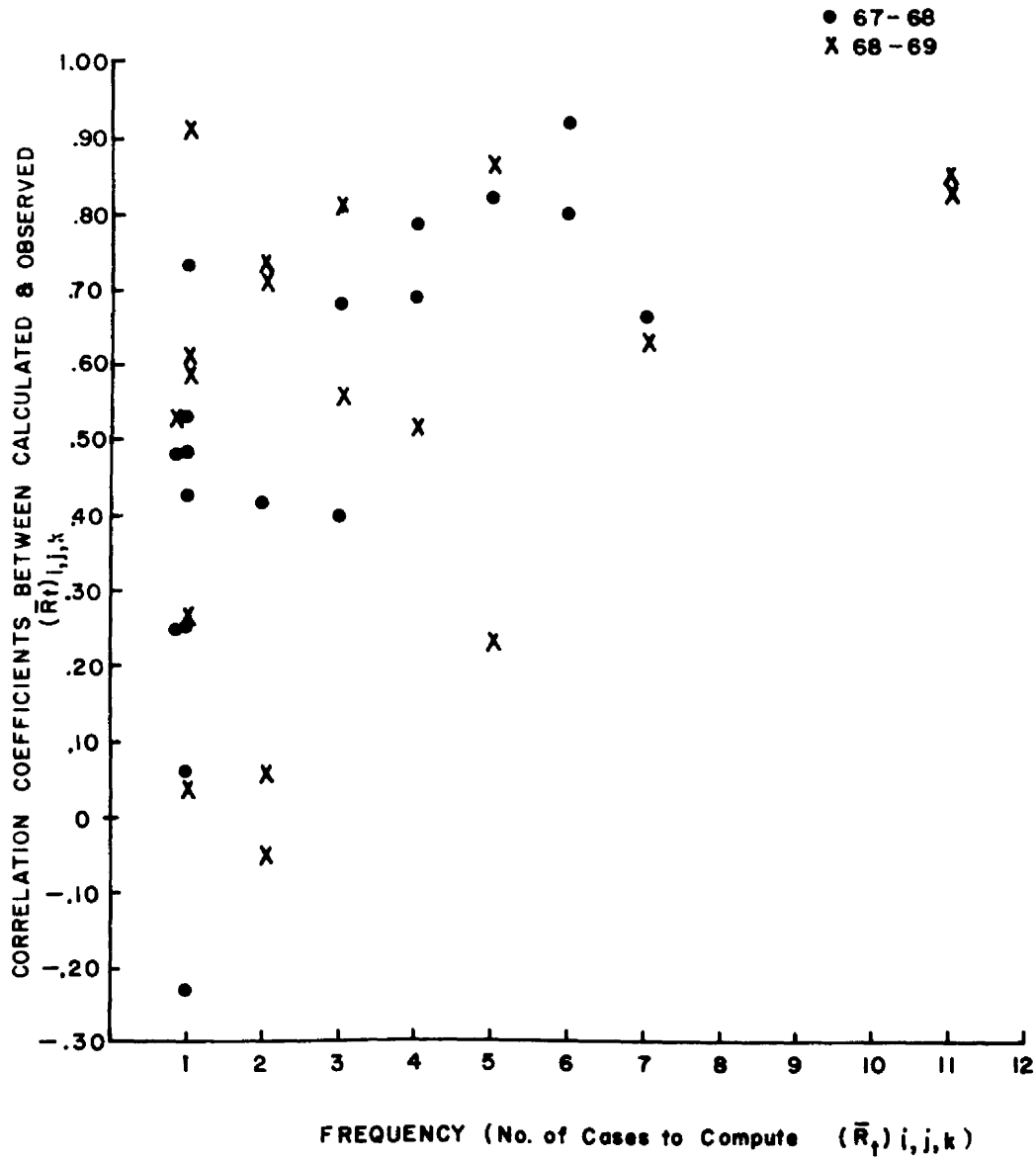

Figure 19. Scatter plot of number of "Precipitation Days" used to compute $(\bar{R}_t)_{i,j,k}$ (by regression equations from Section 4.2.2) vs. correlation coefficients between calculated and observed $(\bar{R}_t)_{i,j,k}$. Note the direct proportionality of correlation coefficient to number of "Precipitation Days".

large scale influences are at work to substantially contribute to or detract from the overall magnitude of precipitation.

A case in point is direction 2, speed 2 for 1968-69 (Figure 15) when the regression equation severely overforecast precipitation. One of the probable large scale influences contributing to this light precipitation was (the suspected presence of)negative horizontal wind shear of the upper level wind field (and therefore, large scale subsidence). Both Rasmussen (1963) and Rangno of EG&G (1970) have emphasized the necessity for positive (cyclonic) horizontal shear of the 500 mb wind over the study area for precipitation occurrence. Another variant is simply the timing of movement of the moist air into the area. Possibly both effects can actually be seen by close scrutinity of Figure 15 in combination with Figure 18. It is at least notable that stations in the northwest part of the region and/or near the San Juan crest show the least deficit in observed versus calculated precipitation values. This is also true in Figure 16, while Figures 14, and 17 show just the opposite effect with high relative precipitation values over the south or southeast part.

4.3.2 Test Points Near Silverton

Silverton rests in a local area of extremely complex terrain. Yet, this study attempts to correlate precipitation to terrain slope features by computing mean values of elevation (and then differencing those to obtain slope) using only three data points over an ever-widening arc with distance from the station (Figure 4). Therefore, in order to determine the validity of (1) the general regression equations for other points within the area of study and (2) the Silverton equation

for points in its immediate vicinity two points only 5 km from Silverton were chosen and their elevation and slope values computed.

These values were input to the appropriate regression equations. The envelope of reasonable calculated values was deemed to range from 50% to 200% of the Silverton observed precipitation for Test Point 1 (with similar terrain profile to Silverton) while for Test Point 2 (on a mountain top 4,000 ft. higher than Silverton) the range was set at 50% to 300%. These ranges were selected based on winter field project experience at several locations in the Colorado Rockies and are documented by reference to Rhea, et al. (1969).

As can be seen, The calculations using the equation set for speed and direction held constant (Section 4.2.1) for both test points near Silverton generally fell within reasonable range of the observed Silverton precipitation. On the other hand, negative precipitation values were calculated for several direction categories from the Silverton regression equation (Section 4.2.5) using test point terrain factors and are meaningless. In truth, the overall seasonal average precipitation likely averages 1.5 to 2.5 times as great for Test Point 2 as for Silverton. Test Point 1 probably receives seasonal average precipitation amounts within ±30% of the Silverton mean value.

4.3.3 Steamboat Springs Test

A test for applicability of the resulting regression equations in other geographic areas was made using Steamboat Springs slope

and elevation factors as independent variables for input to the equations. Steamboat Springs is located roughly 180 nautical air miles north-northeast of the main area of study (Figure 3). Thus, Grand Junction 700 mb wind should have the same degree of validity for Steamboat as for the study area.

Calculated negative values of precipitation at Steamboat in relation to the station terrain profiles (and observed precipitation values) point up the virtual lack of applicability of the exact set of San Juan regression equations (from Section 4.2.1 holding speed and direction constant) for this point. On the other hand, calculations from the general regression equation of Section 4.2.3 at least trended correctly in relation to observed Steamboat precipitation.

In fact, a closer look at these calculations from the general regression equation in Figure 20 yields several interesting inferences. First of all, considering that the correlation coefficient associated with the historical data on which the regression equation was based was only 0.68, the visual correlation between calculated and observed Steamboat Springs values is surprisingly high. Secondly, the calculated $(\overline{R}_t)_{i,j,k}$ values are systematically low for most direction categories. The very high correlation within a given direction category for differing wind speeds (see, for instance, directions 2, 4, 5 and 6) implies considerable physical realism in the general regression equation, but cautions that calibration to fit specific local terrain peculiarities is required to adjust the magnitude of calculated values.

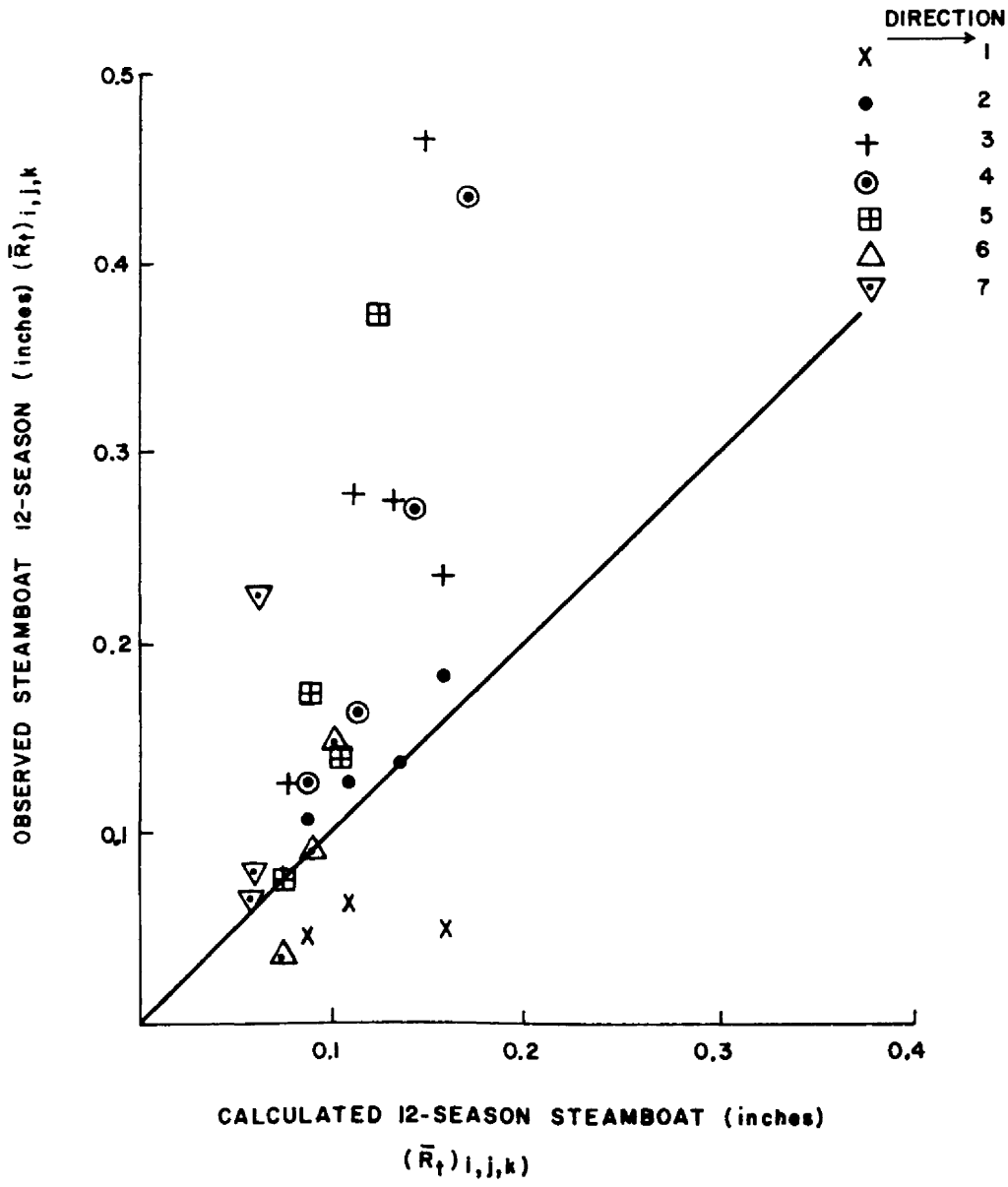

Figure 20. Scatter plot of calculated vs. observed 12-season $(\bar{R}_t)_{i,j,k}$ for Steamboat Springs. Calculations were made from the general regression equation of Section 4.2.3 (with no attempt to isolate the non-orographic precipitation components.)

The over-prediction for direction 1 (175-204°) is consistent with the observational fact that for this wind direction the general area coverage and intensity of (non-orographic) precipitation is much lighter for the Steamboat Springs area than for the section of southwest Colorado where the regression equation (using $\overline{R}_t$ instead of $\overline{R}_o$) was derived.

4.4 Other Tentative Studies

4.4.1 Saturated Layer Depth Variations

This study has to this point ignored variations in saturated layer depth ($\int_P dP$) and duration ($\int_t dt$) even though they are indicated to be potentially very important from Equation (3.7) in Section 3.1.3. This has been done largely because of the lack of knowledge of such variations which can be determined directly from the original data sources used. This section briefly considers variations in $\int_P dP = \Delta P$.

It was assumed for argument that due to the passage of migratory waves and their attendant wind fields and vertical motions there should be an average systematic decrease in ΔP with veering wind. For south-southwest and southwest 700 mb wind, (i=1+2) the cloud depth was estimated at 275 mb (extending from 725 mb to 450 mb) which is similar to that estimated by Chappell (1970). For north-northwest through north-northeast 700 mb winds (i=6+7) it was estimated at 125 mb (from 725 to 600 mb) partially due to observation and also as an estimate of orographic vertical wave length to the first zone of negative vertical motion (Willis, 1970) for stably stratified flow. For lack of any better approximation a linear change in ΔP was assumed between these direction extremes.

Now from the early part of the study described in Section 4.2.4, the slope of the visual best fit regression lines from scatter plotting $(\bar{R}_t)_{i,j,k}$ vs. $\nabla z_{i,k,3}$ (one line for each direction category) decreased as shown by example in Figure 10 as wind direction became more westerly and northerly. (Another way of saying this is that the inter-station range of $(\bar{R}_t)_{i,j,k}$ was lower for more westerly and northerly directions.) Reference to equation (3.7) for orographic precipitation shows that regression line slope (obtained from Figure 10) should be proportional to the quantity:

$$\int_P \int_t |\bar{\vec{V}}|_{700} \left(\overline{\frac{\partial q_s}{\partial z}}\right)_{700} dt\, dP$$

In the early study of Section 4.2.4 for which the Figure 10 scatter plot series were constructed $|\bar{\vec{V}}|_{700}$ was constant and $\int_t dt$ was assumed to always be 24 hours. Therefore,

$$\text{regression line slope (from Figure 10)} \propto \left(\overline{\frac{\partial q_s}{\partial z}}\right)_{700} \Delta P$$

Figure 21 shows the surprisingly high correlation of $\Delta P \cdot \left(\frac{\partial q_s}{\partial z}\right)_{700}$ to regression line slope. This implies the feasibility of refining this study to include more realistic estimates of ΔP.

4.4.2 Duration Variability

Tabulated along with the original daily data was 700 mb temperature-dewpoint spread (dewpoint depression) as a rough indication of humidity. From forecasting experience in western Colorado it can generally be safely stated that little if any precipitation will occur (at altitudes below 11,000 ft. MSL at least) if the spread exceeds 8°C. This is a liberal estimate of delineating moist from dry air, and 5°C is frequently better. However, using a dewpoint depression of >8°C as

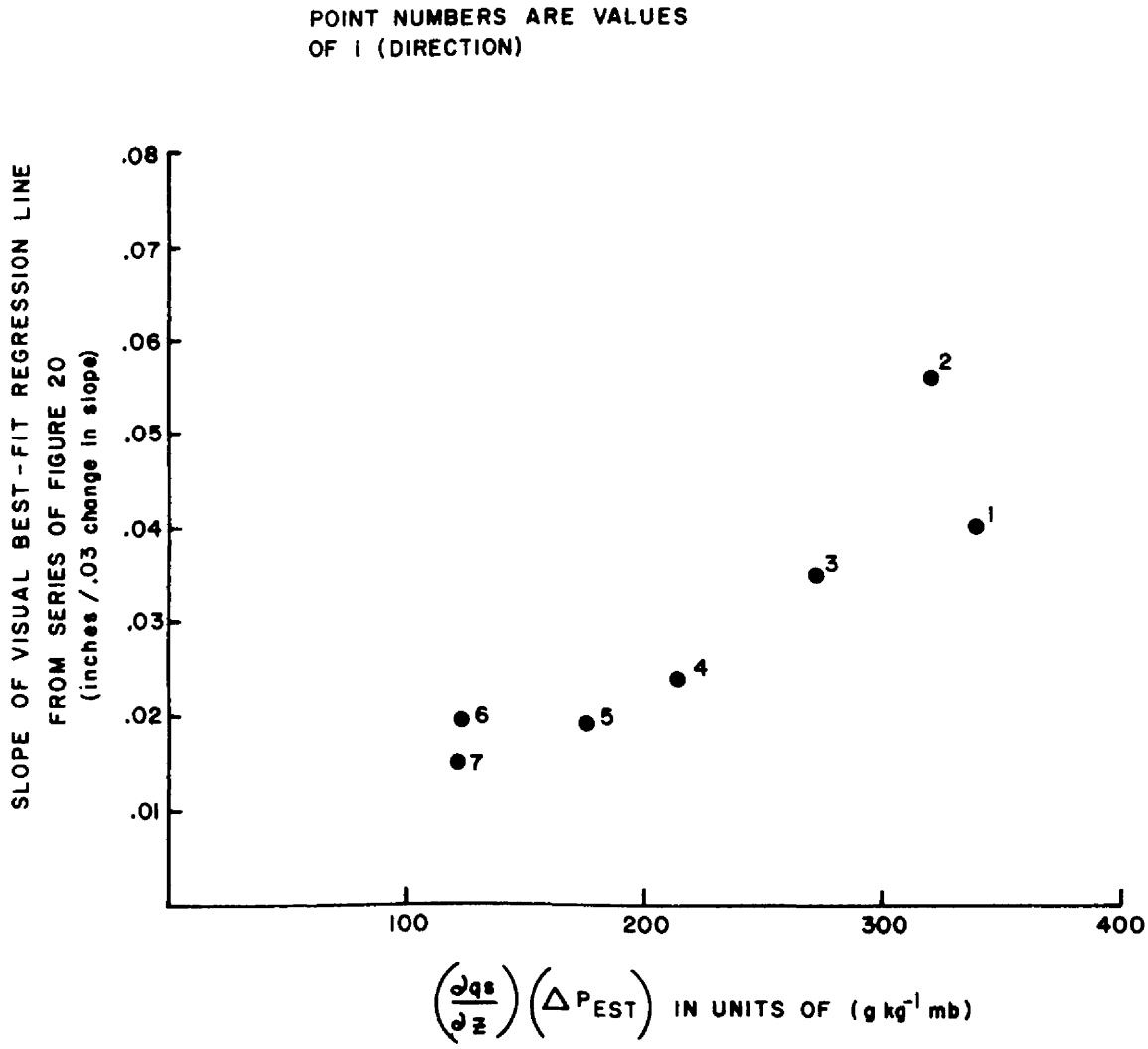

Figure 21. Verification of the expected effect of systematic variations in estimated mean cloud depth (ΔP_{EST}). See Section 4.4.1 of text for details.

the definition of dry, non-precipitating conditions, a duration stratifying factor was applied to the original daily data comprising the sample from which $(\overline{R}_t)_{3,2,k}$ (i.e., for the west-southwest, medium speed data set) values were computed. The factor, t, was defined as 3/3 when all three map times had dewpoint depressions of $\leq 8°C$, 2/3 for 2 of the maps with this condition, 1/3 for 1 and 0 if all three maps exhibited >8°C depressions. Values of t-factor were thus computed. Next the regression equation for i = 3, j = 2 from Section 4.2.1 was invoked but calculated values were first multiplied by the t-factor and then scatter-plotted opposite observed values (Figure 22). It should be pointed out that the five stations with measurable observed precipitation for t = 0 are all located in the northwest part of the region and/or very near the ridge crest. Results strongly suggest that further refinement of this study to include variable duration could lead to reasonable quantitative short-term predictors.

4.4.3 Non-Orographic Precipitation

As mentioned in Section 4.2.4, an estimated non-orographic component $(R_d + R_c)_{i,j,k}$ of precipitation was isolated in an early part of the study. Through the vorticity and divergence theorems this component should be directly proportional to values of $\dot{\zeta} \cdot (\frac{\partial qs}{\partial z}) \cdot \Delta P$ where $\dot{\zeta}$ is the time rate of change in absolute vorticity. Vorticity charts were available on microfilm for study from 1961 and later. Unfortunately they only overlap approximately half of the original study data. However, values of maximum 12 hour vorticity change within the 24 hour period of concern were calculated by Rangno (EG&G, 1970) and mean values of $\dot{\zeta}_{max}$ computed for each direction category. The resulting scatter plot of $\dot{\zeta} \cdot (\frac{\partial qs}{\partial z}) \cdot \Delta P$ vs. $(\overline{R}_d + \overline{R}_c)_{i,j,k}$ in Figure 23 again implies

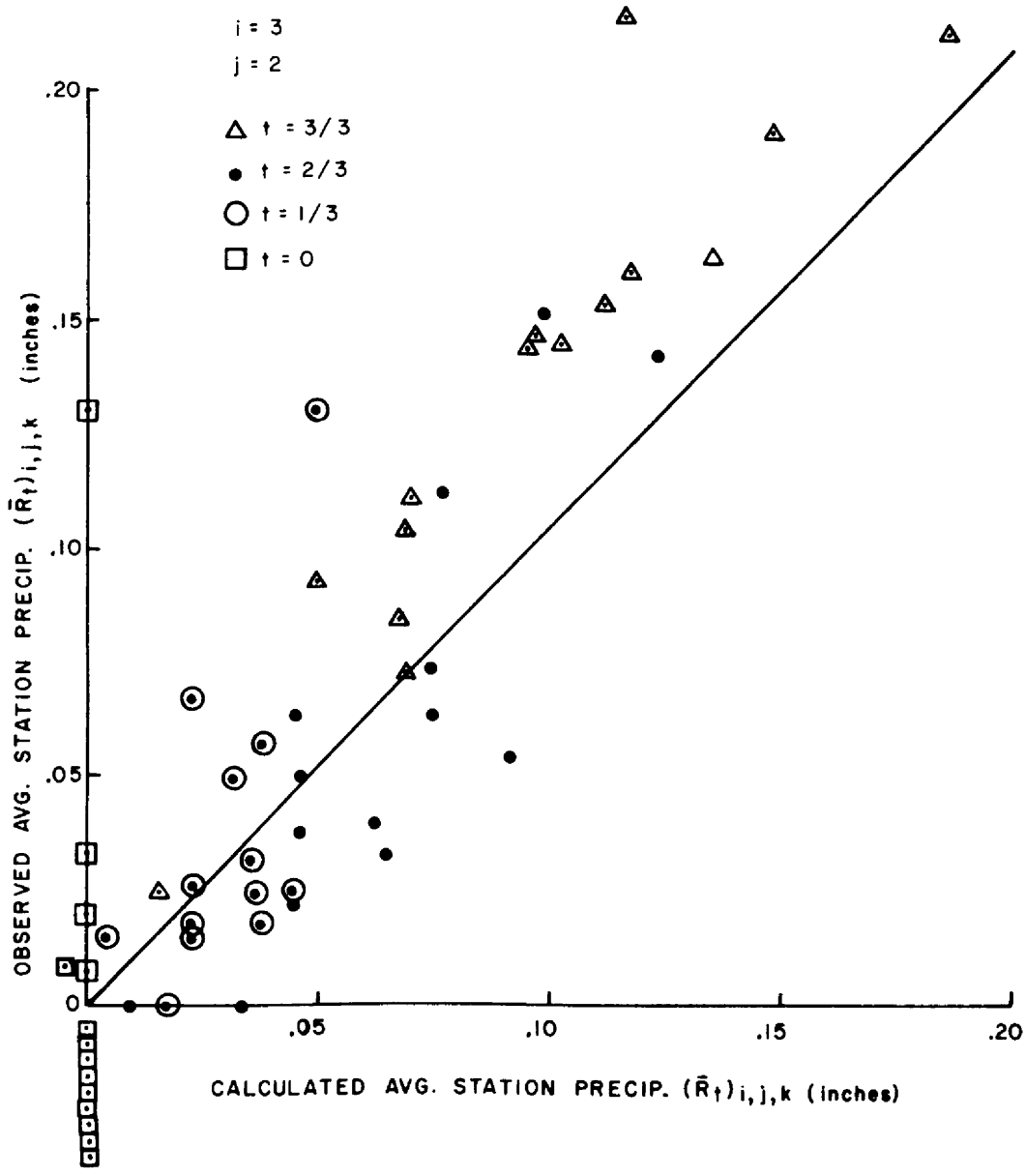

Figure 22. Illustrations of the effect of variable duration of moist air on calculated and observed 24 hour precipitation. See Section 4.4.2 of text for details.

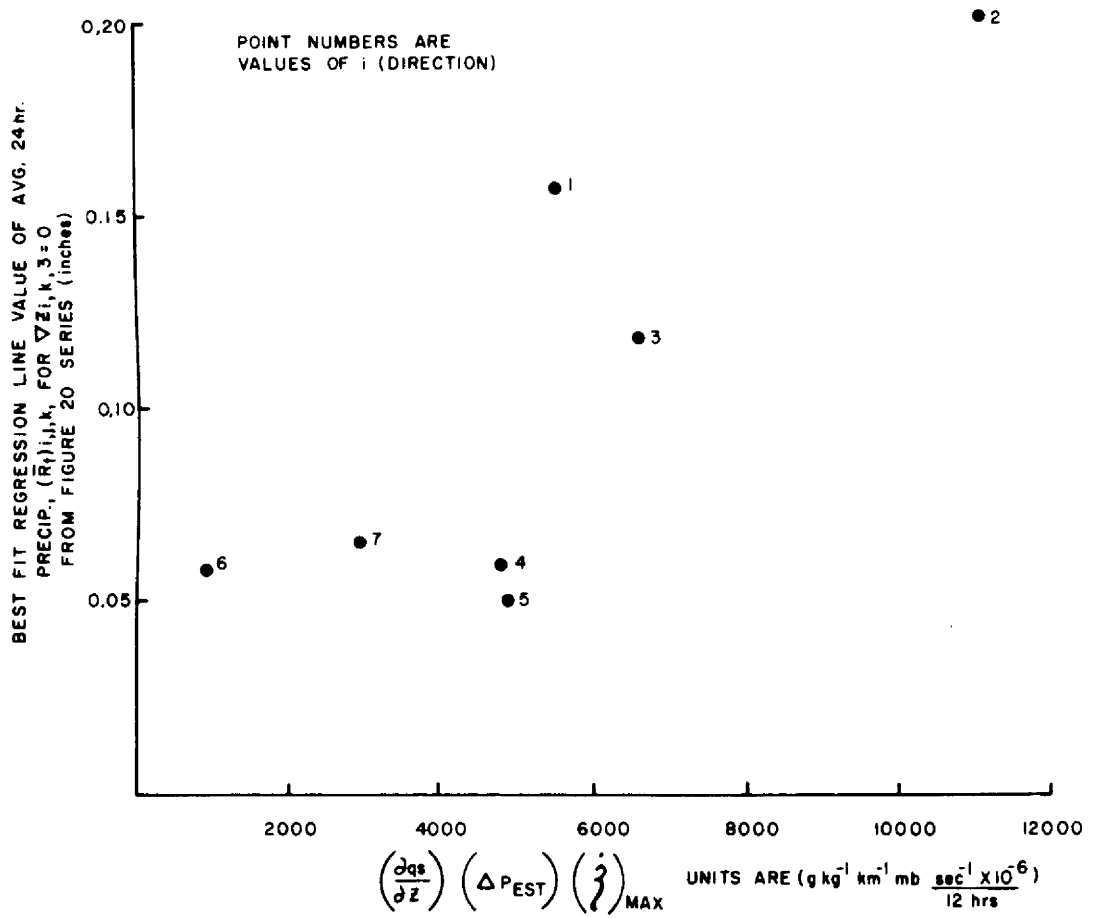

Figure 23. Illustration of the relationship between estimated non-orographic precipitation (vertical axis) and large-scale vertical motion factor (horizontal axis). See Section 4.4.2 of text for details.

the feasibility of refining the study to isolate and take into account the non-orographic component to arrive at a useful estimate of total precipitation.

5.0 SUMMARY AND CONCLUSIONS

The primary objective of this study was to gain knowledge of the terrain (orographic) effect on winter precipitation in a mountainous region. It pursued this knowledge by systematically studying average 24 hour precipitation at given points in relation to the products of wind-direction dependent terrain slope factors, wind speed, and the local vertical lapse of saturation mixing ratio, $(\frac{\partial qs}{\partial z})$.

Standard linear multiple regression techniques were used to develop regression equations for station precipitation, using a 12 winter season record for fifteen (15) NOAA climatological stations in southwestern Colorado, and area topographic maps to determine terrain features (for independent variables). 700 mb wind directions, speeds, temperatures and dewpoints for Grand Junction, Colorado were tabulated. Wind direction and speed stratifications therefrom were applied to the precipitation data set (which was comprised of days on which at least one station received measurable precipitation). Estimates of $(\frac{\partial qs}{\partial z})$ were obtained for the 700 mb level using the Grand Junction 700 mb temperature.

Two winter seasons (November-March, 1967-68 and 1968-69) of precipitation data were used to check the ability of the derived multiple linear regression equations to specify both station total seasonal precipitation and sub-total, within given speed and direction categories. The more general applicability of these equations was also tested by selecting two points within 5 km of one of the original data stations. Their terrain slopes and elevation factors were computed and used as independent variables to obtain predicted values of test point precipitation, which were then compared to nearby readings from the

original data site. Applicability to more distant geographic areas was tested similarly by selecting a station some 200 miles distant and treating it in the same manner as the above two test points.

The bulk of the study ignored variations in (1) estimated mean cloud depth, (2) duration (within the 24 hour period) and (3) nonorographic influences on precipitation. Brief attention to such variations was given in Section 4.4.

Conclusions that can be drawn from the study include:

(1) When viewed in relation to major terrain features and 700 mb wind direction, the contour patterns of the dimensionless normalized 24 hour average precipitation ratios, $(\bar{R}_t)_{i,k}/(\bar{R}_t)_k$, plainly showed the strong effects of upslope/downslope terrain patterns on this relative precipitation. [NOTE: $(\bar{R}_t)_{i,k}$ is the 12-season November - March average 24 hour precipitation for point k occurring within a 30 degree sector of 700 mb 24 hour average wind direction (i=1,2...,12), while $(\bar{R}_t)_k$ is overall 12-season November - March average 24 hour precipitation for point k regardless of wind direction.]

(2) Multiple linear regression of the 12-season direction - and speed - stratified average 24 hour precipitation $[(\bar{R}_t)_{i,j,k}]$ for the set of k stations to elevation and the set of terrain slope factors yielded multiple correlation coefficients of 0.80 to 0.98 when the regression analyses were performed holding direction, i, and speed, j, constant [NOTE: Terrain slope was computed over eight distance scales about each station for each wind direction (i) category, and these values were then multiplied by 700 mb wind speed and local vertical change in 700 mb mean saturation mixing ratio]. Highest single correlation (r = 0.70 to 0.85) was generally noted with respect to either the slopes computed over the distance 10 km downwind to 20 km

upwind or 40 km downwind to 40 km upwind. Precipitation was also frequently highly correlated to slope measured over the distance 10 km upwind to 50 km upwind. Correlation to station elevation was generally quite negligible.

(3) When first letting wind speed vary, and then permitting both speed and direction to vary, resulting sets of multiple correlation coefficients became progressively lower but still showed 0.68 for speed and direction both variable with a sample size of 405 (15 precipitation stations, each with averages for 27 combinations of i, (direction) and j, (speed)).

(4) A rough attempt to next isolate an average non-orographic component (by direction category), remove this component from the sample precipitation data and then perform regression analysis for the variable speed and direction total sample yielded only slightly higher correlation ($r = 0.71$).

(5) Regression analyses for individual stations (thus allowing free range of the 27 (i, j) joint stratifications) yielded r-values of 0.51 to 0.98. Stations with the lowest correlations were noted to be topographically most complex or situated in complicated snow crystal "spillover" regions.

(6) Reasonable ability to account for seasonal precipitation (or at least the orographic portion) from the regression equation derived for individual i, j categories and also for individual stations was found by testing the equation for two additional seasons. Correlation between calculated and observed precipitation values for each season and by each method ranged from 0.89 to 0.93. Substantial over or under-prediction sometimes occurred, yet correlation remained high.

This implies systematic variation in large scale influences affecting the total precipitation.

(7) Qualitative applicability of the regression equations derived for all stations by holding direction and speed constant was noted for two test points, each 5 km from one of the original data stations (Silverton). However, virtually no consistent applicability could be seen for either test when using the Silverton regression equation and the terrain factors of the test points.

(8) A test of the applicability of the general regression equation to other geographic areas (using Steamboat Springs located 200 miles north of the main study area) showed good overall correlation of calculated to observed values of precipitation. Observed values were generally considerably higher than predicted. Exceptions to this generalization are partially explicable on the basis of systematic differences in non-orographic precipitation components between the two areas for given wind directions.

(9) Brief tests exploring the feasibility of refining the study toward a short-term predictor of orographic precipitation were all very encouraging. These included briefly relating (1) inter-station range in precipitation for a given speed and direction category to estimated cloud depth, (2) estimated non-orographic precipitation component to average maximum 12 hour vorticity change and (3) variations in observed precipitation at a given station within a given speed and direction category to variations in duration of moist air and the inhomogeneous distribution of moist air across the area of study.

BIBLIOGRAPHY

Berkofsky, L. (1964): The fall-off with height of terrain-induced vertical motions. Journal of Applied Meteorology. Vol. 3, No. 4, pp. 410-414.

Brown, Stanley (1970): Terminal velocity of snow crystals. Master's Thesis, Colorado State University, Atmospheric Science Paper No. 170, May, 1970.

Chappell, C. F. (1970): Modification of cold orographic clouds. Ph.D. Dissertation, Colorado State University, Atmospheric Science Paper No. 173, December, 1970.

Davis, L. G., J. I. Kelley, A. Weinstein and H. Nicolson (1968): Weather modification experiments in Arizona. Department of Meteorology, Pennsylvania State University, 128 pp.

E. G. & G. (1970): Installation and operation of an opportunity recognition and cloud seeding system for operational weather modification research in Colorado: Phase I. Comprehensive field report to Bureau of Reclamation (Contract No. 14-06-D-6963), E. G. & G., Inc., Boulder, Colorado.

Elliot, Robert D. and Einar L. Hovind (1964): On convection bands within Pacific Coast storms and their relation to storm structure. Journal of Applied Meteorology. Vol. II, pp. 143-228.

_____ and Russell W. Shaffer (1962): The development of quantitative relationships between orographic precipitation and air-mass parameters for use in forecasting and cloud seeding evaluation. Journal of Applied Meteorology. Vol. 1, pp. 218-

Hjermstad, L. M. (1970): The influence of meteorological parameters on the distribution of precipitation across central Colorado mountains. Master's Thesis, Department of Atmospheric Science, Colorado State University, Atmospheric Science Paper, No. 163.

Hounam, C. E. (1958): Estimation of average annual rainfall over the Port Phillip region of Victoria. Australian Meteorological Magazine. No. 21, pp. 1-30.

Kusano, K., K. Noguchi and M. Sumino (1957): A practical technique of forecasting orographic precipitation. Journal of Meteorological Research. Tokyo, Vol. 9, No. 11, pp. 811-822.

Marlatt, W. and H. Riehl (1963): Precipitation regimes over the Upper Colorado River. Journal of Geophysical Research. Vol. 68, pp. 6447-6458.

Peck, E. L. and M. J. Brown (1962): An approach to the development of isohyetal maps for mountainous areas. Journal of Geophysical Research. Vol. 67, pp. 681-694.

_____ and P. Williams, Jr. (1962): Terrain influences on precipitation in the intermountains West as related to synoptic situations. Journal of Applied Meteorology. Vol. 1, pp. 343-347.

Rasmussen, James L. (1963): Some aspects of the monthly precipitation over the Colorado River Basin. Colorado State University, Atmospheric Science Technical Paper No. 46, December, 1963.

_____ (1968): Atmospheric water balance of the Upper Colorado River Basin. Colorado State University, Atmospheric Science technical paper No. 121.

Rhea, J. Owen (1967): A weather typing scheme for the Park Range in northwestern Colorado. Presented at the American Meteorological Society conference on weather analysis and forecasting, Fort Worth, Texas, November, 1967.

_____, P. Willis and L. G. Davis. Park Range atmospheric water resources program. Final report to Bureau of Reclamation (Contract No. 14-06-D-5640). E. G. & G., Inc., Boulder, Colorado.

Rogers, Charles Frederick (1970): A mountain precipitation study. Master's Thesis, University of Nevada.

Sarker, R. P. (1967): Some modifications in a dynamical model of orographic rainfall. Monthly Weather Review. Vol. 95, No. 10, pp. 673-684.

Simpson, J., V. Wiggert and T. R. Meer (1968): Models of seeding experiments on supercooled and warm cumulus clouds. Proceedings First National Conference on Weather Modification, Albany, New York, pp. 251-269.

_____ (1970): Cumulus cloud modification: Progress and Prospects. A Century of Weather Progress. 1970, pp. 143-155.

Spreen, William C. (1947): A determination of the effect of topography upon precipitation. American Geophysical Union. Transactions, Vol. 28, No. 2, pp. 285-290.

Weinstein, A. I. and L. G. Davis (1967): A parameterized numerical model of cumulus convection. Department of Meteorology, The Pennsylvania State University, Report No. 11 to National Science Foundation.

Weinstein, A. I. (1968): A numerical model of cumulus dynamics and microphysics. Ph.D. Thesis, Department of Meteorology, Pennsylvania State University.

Willis, Paul T. (1970): A parameterized numerical model of orographic precipitation. Prepared for Bureau of Reclamation (Contract No. 14-06-D-5640), E. G. & G., Inc., Boulder, Colorado.

BIBLIOGRAPHIC DATA SHEET	1. Report No. CSU-ATSP-197	2.	3. Recipient's Accession No.

4. Title and Subtitle

Interpreting Orographic Snowfall Patterns

5. Report Date: January, 1973

6.

7. Author(s): J. Owen Rhea

8. Performing Organization Rept. No.

9. Performing Organization Name and Address

Department of Atmospheric Sciences
Colorado State University
Fort Collins, Colorado

10. Project Task Work Unit No.

11. Contract/Grant No.: 15-1371-113

12. Sponsoring Organization Name and Address

Experiment Station
Administration Building
Colorado State University
Fort Collins, Colorado 80521

13. Type of Report & Period Covered

14.

15. Supplementary Notes

Condensation of author's M.S. Thesis at CSU

16. Abstracts

Winter precipitation in mountainous southwest Colorado was related to terrain slope and elevation by multiple regression. From a 12 season record of 15 daily precipitation stations, the study used only those days with $\geq$ .01 in. at $\geq$ one station. Days used were classed by mean 24 hour 700 mb wind direction and speed. By class, each station's mean 24 hour precipitation was computed as was station slope over 8 distances. These precipitation values were correlated to elevation and to products of terrain slope x 700 mb wind speed x 700 mb mean saturation mixing ratio lapse rate. (Products are simplified factors in an orographic precipitation formula.)

Multiple correlation coefficient ranged between 0.80 and 0.98 for both speed and direction constant and was 0.68 for both variable. Correlation to elevation was negligible. Thus, slope explained most of the areal precipitation distribution. For each of two test years, correlation between computed and observed seasonal precipitation was $\geq$ 0.92. Technique refinement into a short term predictor seems feasible.

17. Key Words and Document Analysis. 17a. Descriptors

snow
orographic snowfall
terrain slope
elevation
wind direction
regression analysis
snowfall distribution
precipitation
precipitation distribution
terrain aspect

17b. Identifiers Open-Ended Terms

17c. COSATI Field/Group

18. Availability Statement	19. Security Class (This Report) UNCLASSIFIED	21. No. of Pages 74
	20. Security Class (This Page UNCLASSIFIED)	22. Price